

# Electromagnetic Baryon Transition Form Factors

---

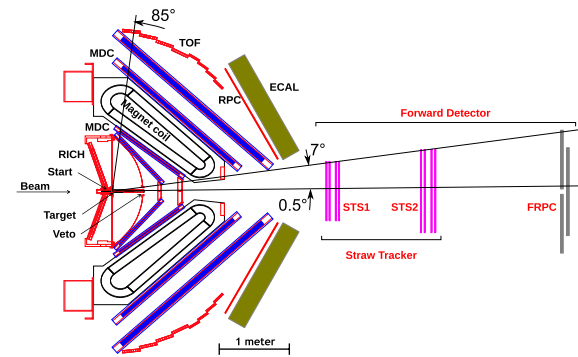
Teresa Peña

In Collaboration with Gilberto Ramalho,  
Gernot Eichmann, André Torcato, Ana Arriaga



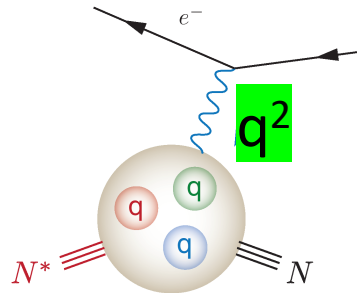
✓ HADES collaboration

Enables studies in the few GeV region;  
probes electromagnetic couplings with  
short-lived QCD systems.



# Electromagnetic Transition form factors (TFF's)

## Baryon resonances transition form factors



CLAS: Aznauryan et al.,  
Phys. Rev. C 80 (2009)

MAID: Drechsel, Kamalov, Tiator,  
EPJ A 34 (2009)

Gernot Eichmann and Gilberto Ramalho  
Phys. Rev. D 98, 093007 (2018)

G. Ramalho, M. T. P. ,  
Prog. Part. Nucl. Phys., (2023)

$$q^2 < 0$$

### Spacelike form factors:

- Structure information: shape, qq $\bar{q}$  excitation vs. hybrid, ...

$$q^2 > 0$$

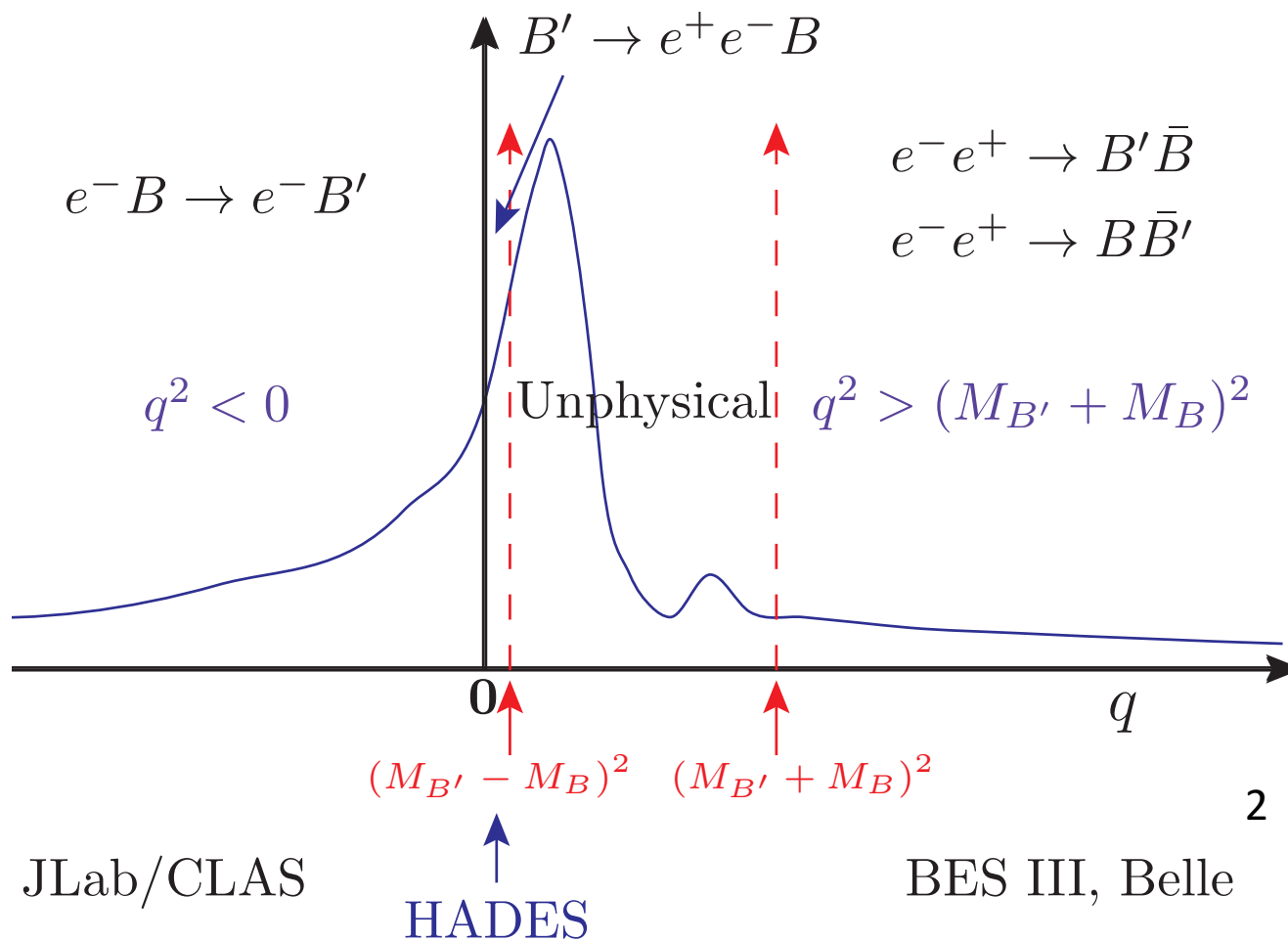
### Timelike form factors:

- Particle production channels, spectroscopy

This talk: our experience

Connect Timelike and Spacelike Transition Form Factors (TFF)

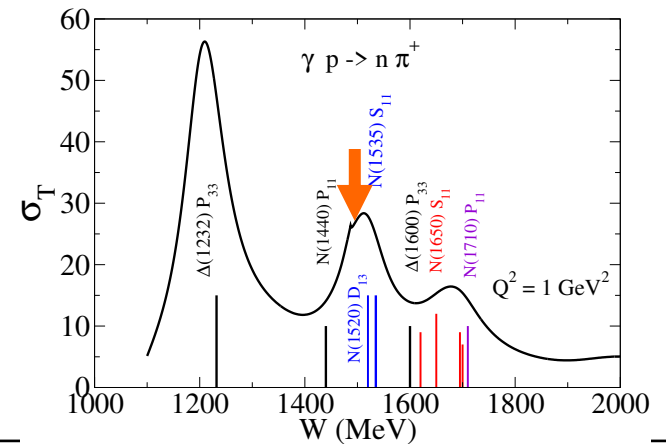
Obtain Baryon-Photon coupling evolution with 4 momentum transfer



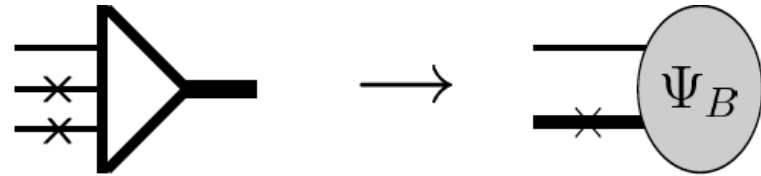
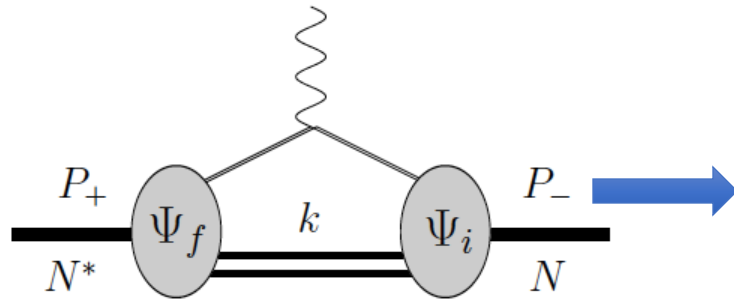


# Baryon resonances S=0 PDG

$I$	$S$	$J^P = \frac{1}{2}^+$	$\frac{3}{2}^+$	$\frac{5}{2}^+$	$\frac{1}{2}^-$	$\frac{3}{2}^-$	$\frac{5}{2}^-$
$\frac{1}{2}$	0	<b>N(940)</b>	<b>N(1720)</b>	<b>N(1680)</b>	<b><u>N(1535)</u></b>	<b><u>N(1520)</u></b>	<b>N(1675)</b>
		<b>N(1440)</b>	$N(1900)$	$N(1860)$	<b>N(1650)</b>	$N(1700)$	
		$N(1710)$			$N(1895)$	$N(1875)$	
		$N(1880)$					
$\frac{3}{2}$	0	<b><math>\Delta(1910)</math></b>	<b><u><math>\Delta(1232)</math></u></b>	<b><math>\Delta(1905)</math></b>	<b><math>\Delta(1620)</math></b>	<b><math>\Delta(1700)</math></b>	$\Delta(1930)$
			$\Delta(1600)$		$\Delta(1900)$	$\Delta(1940)$	
			$\Delta(1920)$				



# E.M. matrix element



$$\int_{k_1 k_2} \equiv \int \frac{d^4 k_1 d^4 k_2}{(2\pi)^6} \delta_+(m_1^2 - k_1^2) \delta_+(m_2^2 - k_2^2)$$

$$= \int \frac{d^3 k_1 d^3 k_2}{(2\pi)^6 4E_1 E_2}$$

$$\int_{sk} = \underbrace{\int \frac{d\Omega_{\hat{\mathbf{r}}}}{4(2\pi)^3} \int_{4m_q^2}^{\infty} ds \sqrt{\frac{s - 4m_q^2}{s}}}_{\int_s} \underbrace{\int \frac{d^3 k}{(2\pi)^3 2E_s}}_{\int_k}$$

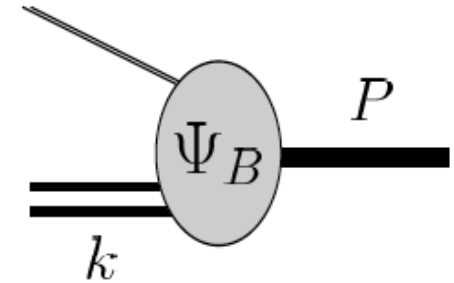
- **For the E.M. matrix element calculation**, the Baryon vertex is integrated over the spectator quarks variables.  
(Covariant Spectator Model, **CST**)

- **A reduced quark - diquark Baryon** wave function is all that is needed; it is phenomenologically constructed.

- ✓ The wf is symmetry based only; not dynamically generated
- ✓ The Diquark is not pointlike; it encloses structure  
Eg. S-wave

■ **Nucleon** wavefunction

- A quark + **scalar**-diquark component
- A quark+ **axial vector**-diquark component



$$\Psi_{N\lambda_n}^S(P, k) = \frac{1}{\sqrt{2}} [\phi_I^0 u_N(P, \lambda_n) - \phi_I^1 \varepsilon_{\lambda P}^{\alpha*} U_\alpha(P, \lambda_n)]$$

$$\times \boxed{\psi_N^S(P, k)}$$

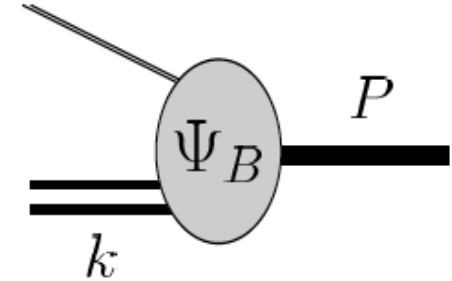
$$U_\alpha(P, \lambda_n) = \frac{1}{\sqrt{3}} \gamma_5 \left( \gamma_\alpha - \frac{P_\alpha}{m_H} \right) u_N(P, \lambda_n),$$

Phenomenological functions  $\psi$

- ✓ The wf is symmetry based only; not dynamically generated
- ✓ The Diquark is not pointlike; it encloses structure  
Eg. S-wave

■ **Nucleon** wavefunction

- A quark + **scalar**-diquark component
- A quark+ **axial vector**-diquark component



$$\Psi_{N\lambda_n}^S(P, k) = \frac{1}{\sqrt{2}} [\phi_I^0 u_N(P, \lambda_n) - \phi_I^1 \varepsilon_{\lambda P}^{\alpha*} U_\alpha(P, \lambda_n)] \times \psi_N^S(P, k)$$

■ **Delta (1232)** “wavefunction”

- Only quark + **axial vector**-diquark term contributes

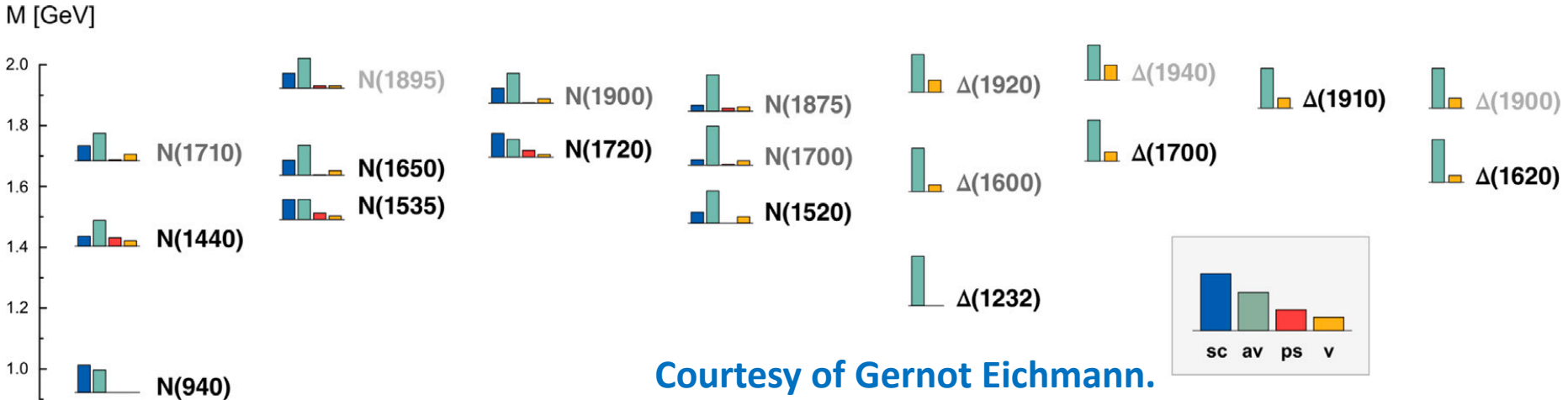
$$U_\alpha(P, \lambda_n) = \frac{1}{\sqrt{3}} \gamma_5 \left( \gamma_\alpha - \frac{P_\alpha}{m_H} \right) u_N(P, \lambda_n),$$

Phenomenological functions  $\psi$

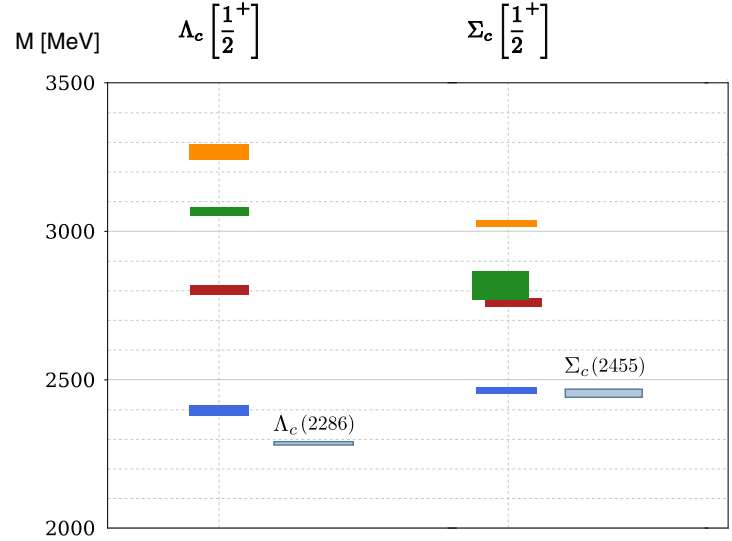
$$\Psi_\Delta^S(P, k) = - \psi_\Delta^S(P, k) \tilde{\phi}_I^1 \varepsilon_{\lambda P}^{\beta*} w_\beta(P, \lambda_\Delta)$$

Dyson–Schwinger methods deciphered puzzle of the low mass of the parity +  $N(1440)$  state relatively to the parity -  $N(1535)$  and  $N(1650)$  states.

The combination of different diquark correlations in baryon structure explained it.



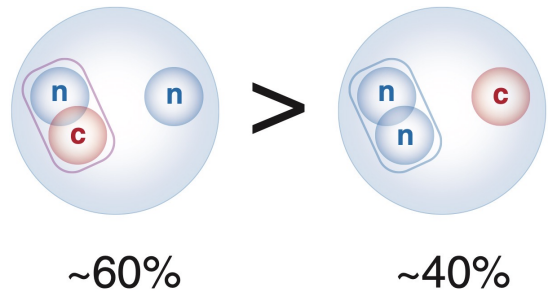
Courtesy of Gernot Eichmann.



**Singly charmed Baryons**

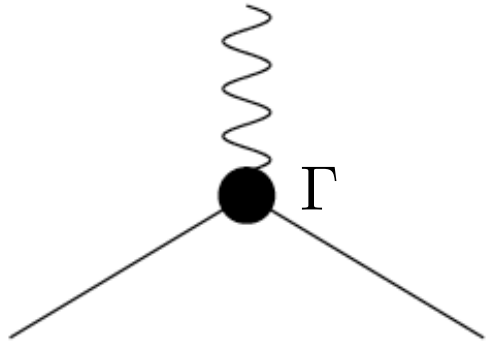
- █ 3rd Excited
- █ 2nd Excited
- █ 1st Excited
- █ Ground
- █ Experiment

$n \rightarrow u, d$



A. Torcato, A. Arriaga, G. Eichmann, M. T. P. *Few Body Syst.* 64 3, 45 (2023)

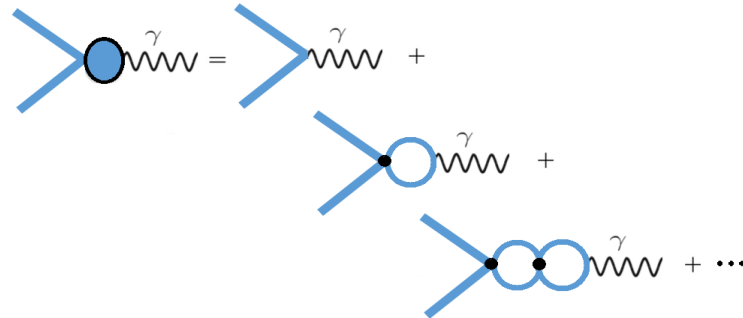
# Quark E.M. Current



quark-antiquark

⊕ gluon dressing

Quark-photon vertex



$$\Gamma_\mu(p, Q) = \gamma_\mu + \int \frac{d^4q}{(2\pi)^4} K(p, q, Q) S(q + \eta Q) \Gamma_\mu(q, Q) S(q - \eta Q)$$

Meson Spectrum is tied to this vertex

Constituent quarks (quark form factors)

$$j_I^\mu = \left[ \frac{1}{6} f_{1+} + \frac{1}{2} f_{1-} \tau_3 \right] \gamma^\mu + \left[ \frac{1}{6} f_{2+} + \frac{1}{2} f_{2-} \tau_3 \right] \frac{i\sigma^{\mu\nu} q_\nu}{2M_N}$$

To parametrize the current we use **Vector Meson Dominance at the quark level**, a truncation to the rho and omega poles of the full meson spectrum contribution to the quark-photon coupling.

**4** parameters

# VMD as link to LQCD

---

**experimental data**  
well described in  
the large  $Q^2$  region.

**VMD**

Take the limit of the physical  
pion mass value

In the current the **vector meson** mass  
is taken as a function of the running  
pion mass.

quark model  
calibrated to the  
**lattice data**

Pion cloud contribution  
negligible for **large pion masses**

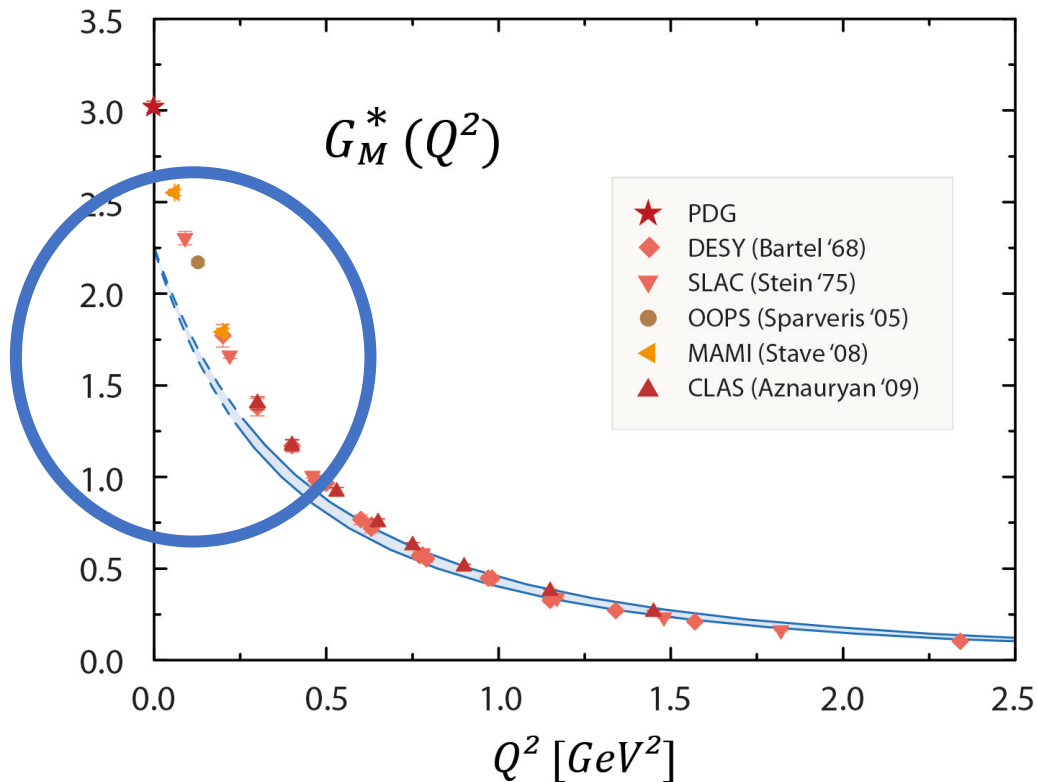


# Model independent feature



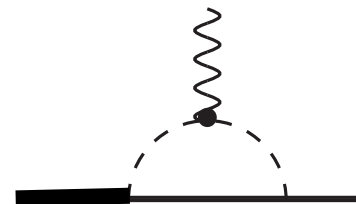
Missing strength of  $G_M$  at the origin is an universal feature, even in dynamical quark calculations.

Eichmann et al., *Prog. Part. Nucl. Phys.* 91 (2016)



Effect of vicinity of the mass of the Delta to the pion-nucleon threshold.

Pion loop effects suppressed for high  $Q^2$   $\frac{1}{Q^8}$





# $N \rightarrow N^*(1520)$ TFFs

$$J^P=3/2^- \quad I=1/2$$

60% decay

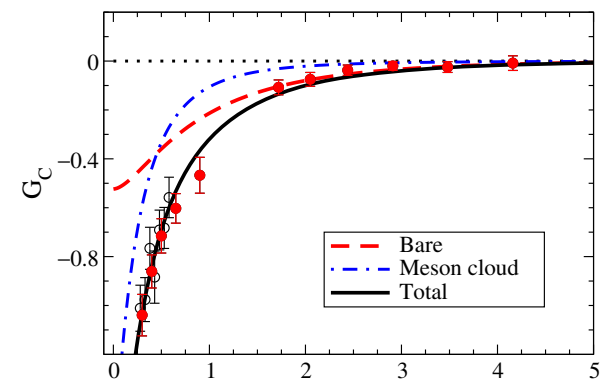
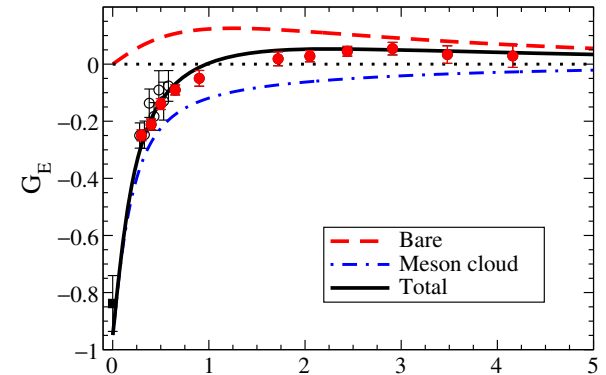
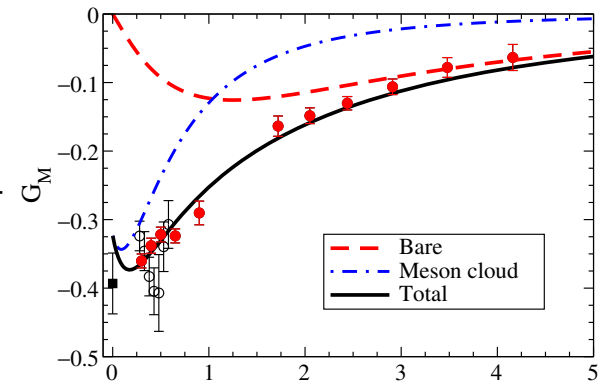
$\pi N$

30% decay to

$\pi \Delta$

- Bare quark model gives good description in the high momentum transfer region.
- For low  $Q^2$ , failure of description hints to meson effects.

Consistent with Aznauryan and Burkert,  
PRC 85 055202 2012 and PDG



G. Ramalho, M. T. P., PHYSICAL REVIEW D 95 014003 (2017)

$Q^2$  (GeV<sup>2</sup>)

# $N \rightarrow N^*(1520)$

---

PDG data at the photon point:

	$A_{1/2}$	$A_{3/2}$	$ A ^2$
$p$	$-0.025 \pm 0.005$	$0.140 \pm 0.005$	$20.2 \pm 1.4$
$n$	$-0.050 \pm 0.005$	$-0.120 \pm 0.005$	$15.7 \pm 1.3$



$$A_{3/2}^V \approx 0.13 ; A_{3/2}^S \approx 0.01 \text{ (GeV}^{-1/2}\text{)}$$

Dominance of iso-vector channel concurs  
to the interpretation of low  $Q^2$  effects as “pion cloud effects”

# $N \rightarrow N^*(1535)$ TFFs

$J^P=1/2^- \quad I=1/2$   
 $\sim 50\%$  decay to  $\pi N$   
 $\sim 50\%$  decay to  $\eta N$

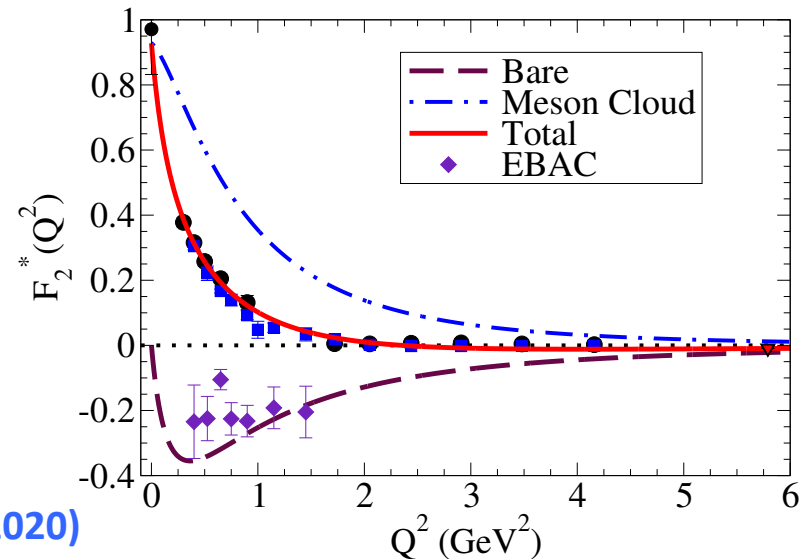
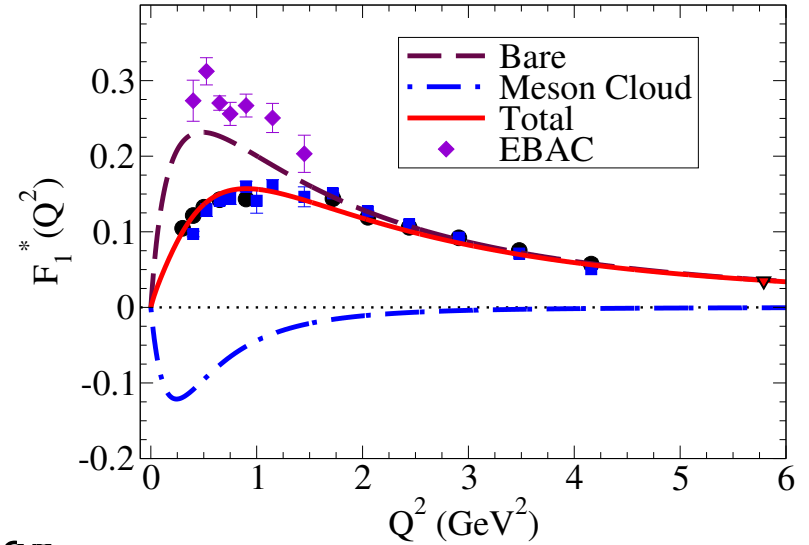
$$J^\mu = \bar{u}_R \left[ F_1^* \left( \gamma^\mu - \frac{\not{q} q^\mu}{q^2} \right) + F_2^* \frac{i\sigma^{\mu\nu} q_\nu}{M_N + M_R} \right] \gamma_5 u_N$$

- Again good agreement of bare quark core with data in the large  $Q^2$  region.
- It dominates  $F_1^*$  for large  $Q^2$
- Meson effects in  $F_2^*$  extend to high  $Q^2$  region.

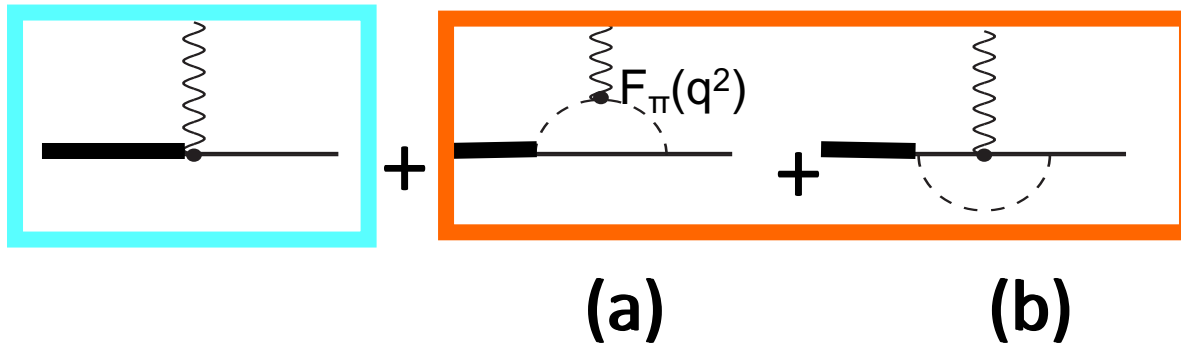
$$A_{1/2}^V(0) = 0.090 \pm 0.013 \text{ GeV}^{-1/2}$$

$$A_{1/2}^S(0) = 0.015 \pm 0.013 \text{ GeV}^{-1/2}$$

Effect from the  $\eta N$  together with  $\pi N$  channel



# Extension to the Timelike region



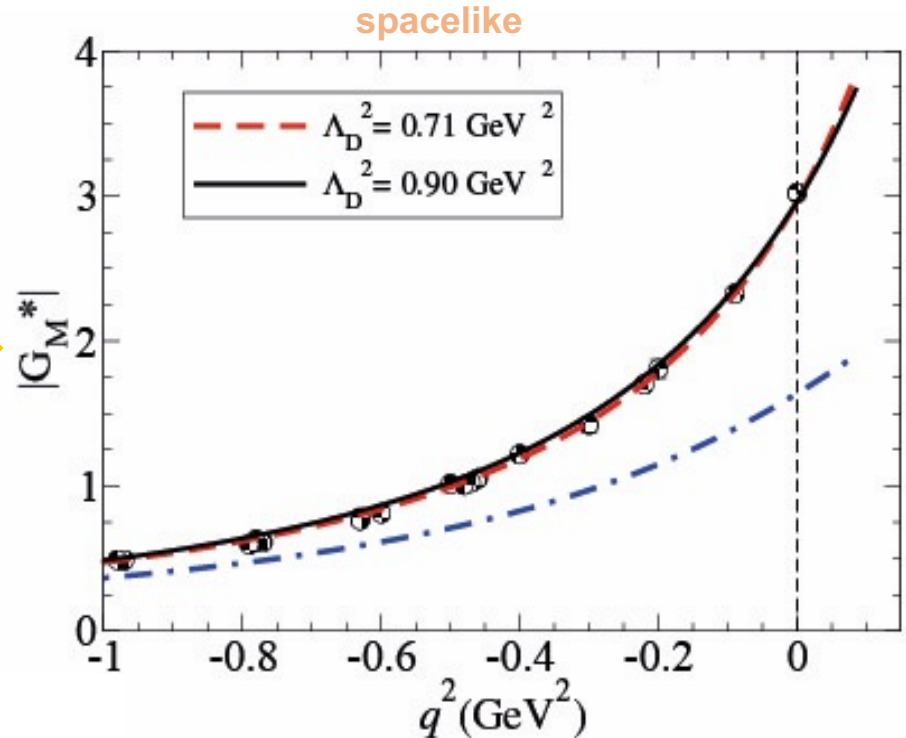
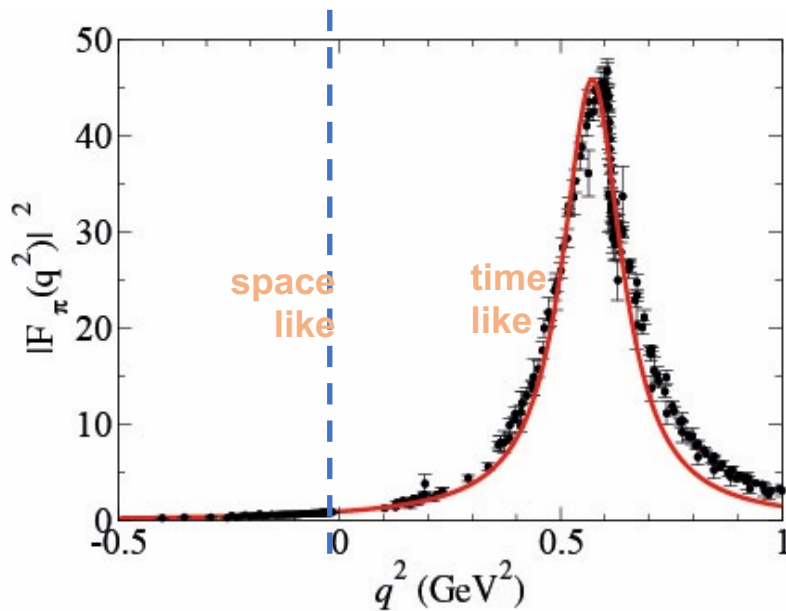
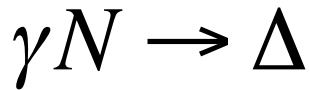
The residue of the pion from factor  $F_\pi(q^2)$  at the timelike  $\rho$  pole is proportional to the  $\rho \rightarrow \pi\pi$  decay

Diagram (a) related with pion electromagnetic form factor  $F_\pi(q^2)$

# Extension to the Timelike region

# $\Delta(1232)$ Dalitz decay

Ramalho, Pena, Weil, Van Hees, Mosel, Phys.Rev. C93 033004 (2016)



Parametrization of pion Form Factor

$$F_\pi(q^2) = \frac{\alpha}{\alpha - q^2 - \frac{1}{\pi} \beta q^2 \log \frac{q^2}{m_\pi^2} + i\beta q^2}$$

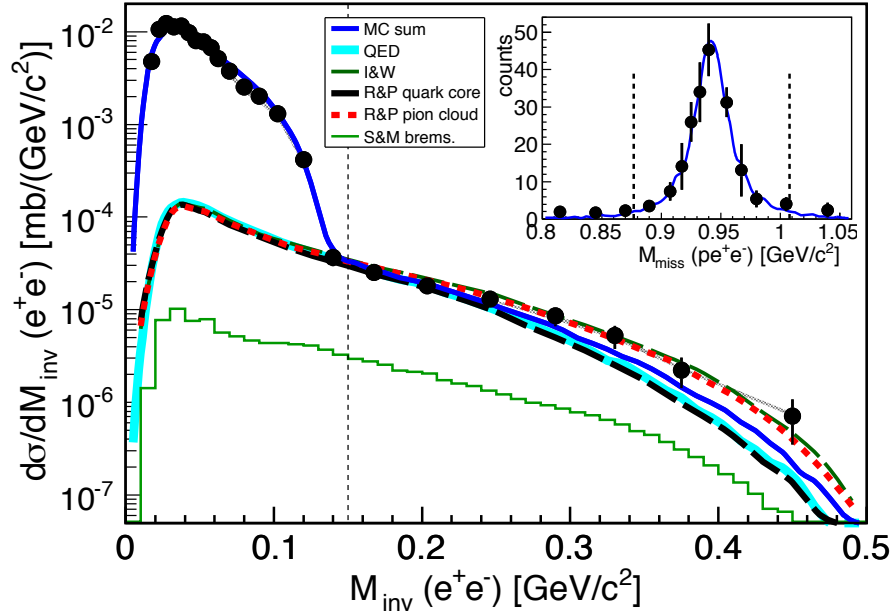
$\alpha = 0.696 \text{ GeV}^2$   
 $\beta = 0.178$

TFF restricted to the kinematic region that depends on the resonance mass  $W$ .

# Dilepton mass spectrum

$\Delta(1232)$  Dalitz decay

HADES Collaboration, Phys.Rev. C95 0652205 (2017)  
proton-proton collisions @1.25 GeV



True CST prediction:  
Red line

Signature of adequate TFF form factor  $q^2$  dependence

$\Delta$  Dalitz decay branching ratio extracted  $4.19 \times 10^{-5}$

$\Gamma(pe^+e^-)/\Gamma_{total}$

VALUE (units  $10^{-5}$ )

$4.19 \pm 0.34 \pm 0.62$

DOCUMENT ID

<sup>1</sup> ADAMCZEW... 17

$\Gamma_5/\Gamma$

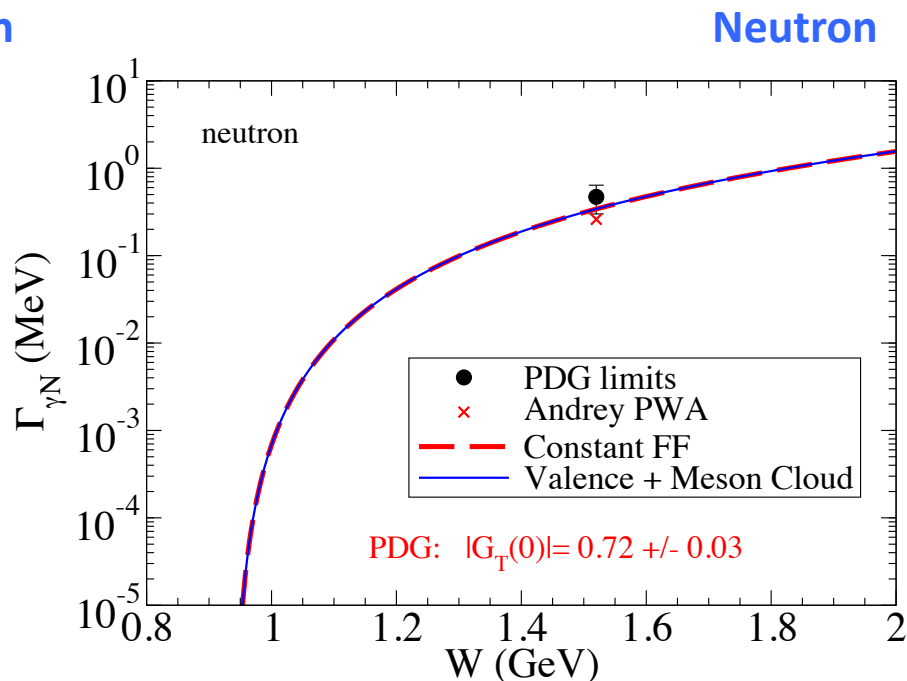
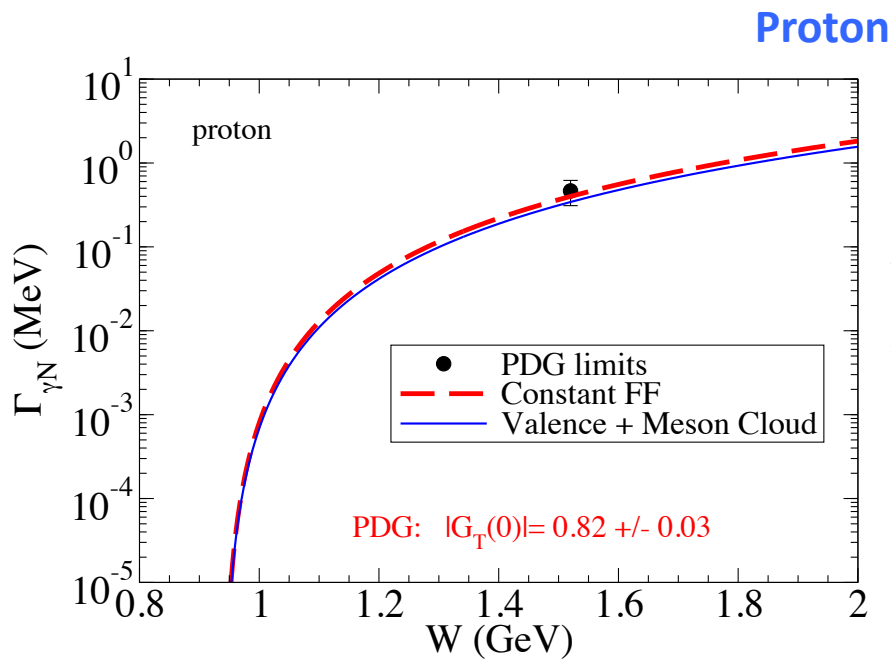
<sup>1</sup> The systematic uncertainty includes the model dependence.

Entry in PDG

The obtained  $\Delta$  Dalitz branching ratio at the pole position is equal to  $4.19 \times 10^{-5}$  when extrapolated with the help of the Ramalho-Peña model [27], which is taken as the reference, since it describes the data better. The branching ratio

# Radiative decay widths

$N^*(1520)$   $J^P=3/2^-$   $I=1/2$   
60% decay  $\pi N$   
30% decay to  $\pi \Delta$



G. Ramalho and M.T. P. Phys. Rev. D 95, 014003 (2017)

Result Consistent with PDG value for  $\gamma N$  decay width.

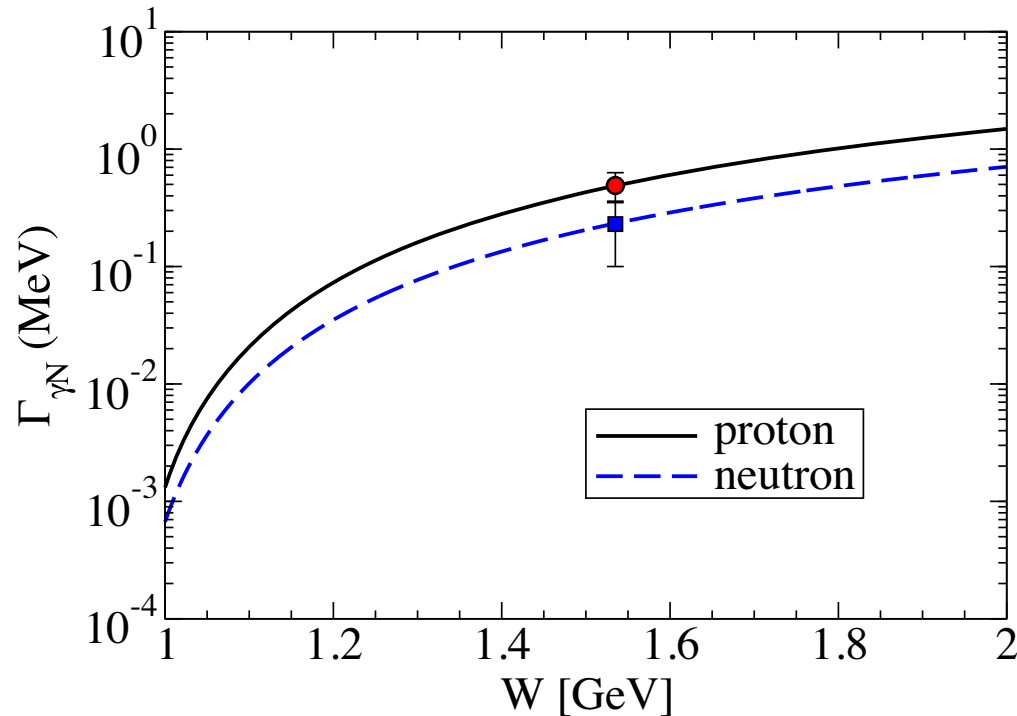
# Radiative decay widths

$N^*(1535)$

$J^P=1/2^- \quad I=1/2$

$\sim 50\%$  decay to  $\pi N$

$\sim 50\%$  decay to  $\eta N$



G. Ramalho and M.T. P. Phys.Rev.D 101 (2020) 11, 114008, (2020)

Different results for proton and neutron electromagnetic widths due to iso-scalar term in the eta meson cloud.

Timelike results give information on the neutron.

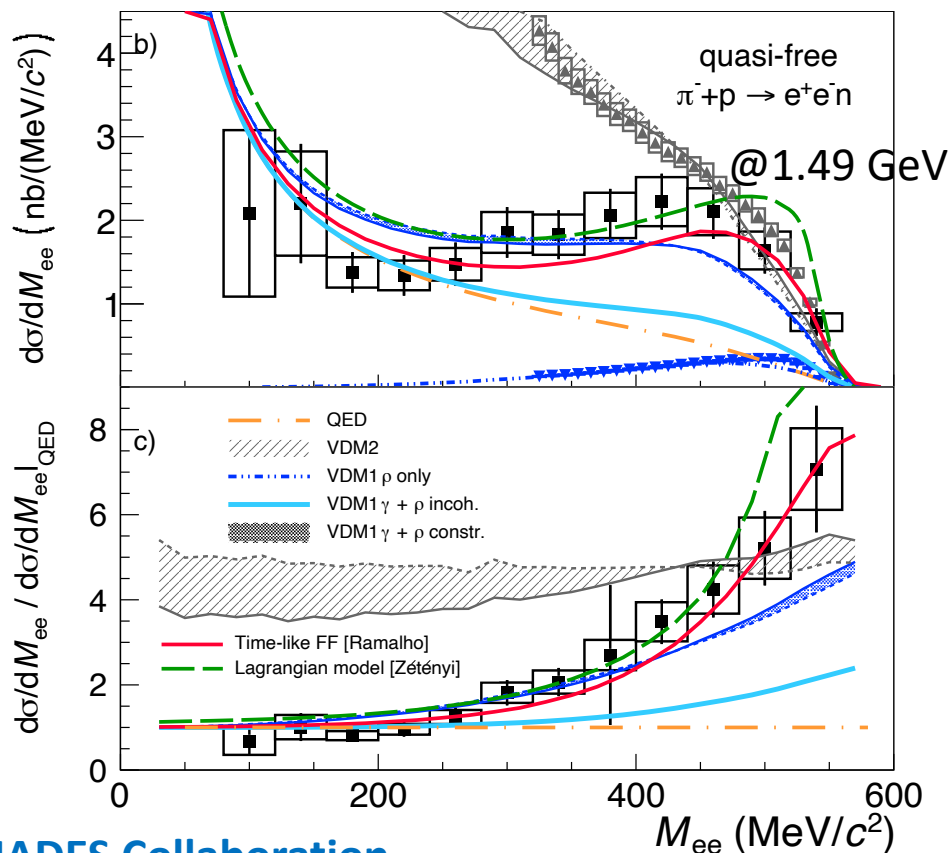
	$A_{1/2}(0)$ [GeV $^{-1/2}$ ]		$\Gamma_{\gamma N}$ [MeV]		
	Data	Model	Estimate	PDG limits	Model
$p$	$0.105 \pm 0.015$	0.101	$0.49 \pm 0.14$	0.19–0.53	0.503
$n$	$-0.075 \pm 0.020$	-0.074	$0.25 \pm 0.13$	0.013–0.44	0.240



# Dilepton mass spectrum

$N^*(1520) + N^*(1535)$   
Dalitz decay

True CST prediction: Red line



Simulations based on the CST model (**red line**) for these resonances also give a satisfactory description of the data.

Below 200 MeV/c<sup>2</sup>, data agrees with a pointlike baryon-photon vertex (**QED orange line**).

At larger invariant masses, data is more than 5 times larger than the pointlike result, showing a strong effect of the transition form factor evolution.

**HADES Collaboration**

“First measurement of massive virtual photon emission from  $N^*$  baryon resonances” e-Prints: 2205.15914 [nucl-ex], 2022 + 2309.13357 [nucl-ex], 2023

# Extension to the Strange Baryon Sector

Extend the parametrization of the e.m. current to the valence quark d.o.f of the **whole** baryon octet.

$$j_i = \frac{1}{6} f_{i+} \lambda_0 + \frac{1}{2} f_{i-} \lambda_3 + \frac{1}{6} f_{i0} \lambda_s$$

$$\lambda_0 = \begin{pmatrix} 1 & 0 & 0 \\ 0 & 1 & 0 \\ 0 & 0 & 0 \end{pmatrix}, \quad \lambda_3 = \begin{pmatrix} 1 & 0 & 0 \\ 0 & -1 & 0 \\ 0 & 0 & 0 \end{pmatrix}$$

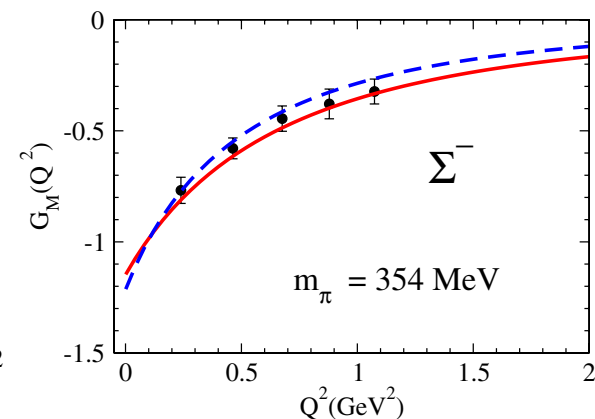
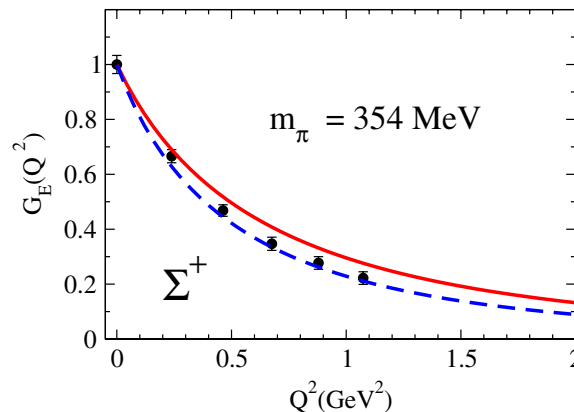
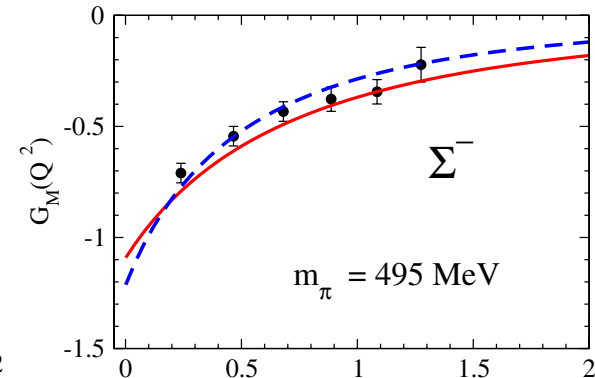
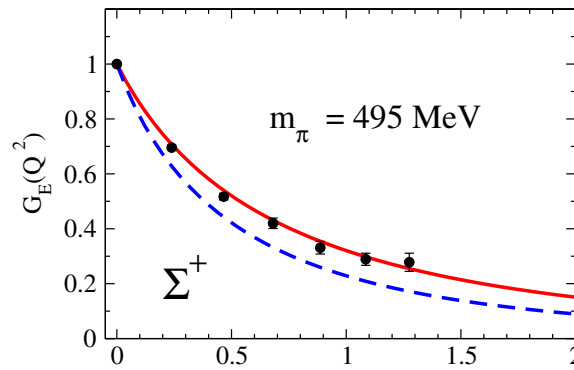
$$\lambda_s = \begin{pmatrix} 0 & 0 & 0 \\ 0 & 0 & 0 \\ 0 & 0 & -2 \end{pmatrix}$$

Parameters determined by a **global fit** to octet baryon lattice data for the e.m. form factors and physical magnetic moments.

**Lattice data:**  
**H.W. Lin and K. Orginos,**  
**Phys. Rev. D 79, 074507 (2009).**

Two examples:

**Red line:** lattice  
**Blue line:** physical regime



**G. Ramalho and K. Tsushima, PRD 84, 054014 (2011)**

# Post 2020 Hyperon data evolution

	$G$	$\frac{G_E}{G_M}$	$\Delta\Phi$	Experiment	$q^2$ range (GeV <sup>2</sup> )
$\Lambda$	✓			BESIII23 [13]	5.0–8.7
	✓			BESIII21 [16]	12.3–21.2
	✓			BaBar06 [8], CLEO [31, 32]	
		✓	✓	BESIII22 [15]	14.2
		✓	✓	BESIII23 [14]	13.8 †
	✓	✓	✓	BESIII19 [22]	5.7
	✓	✓		BaBar07 [9]	
$\Sigma^+$	✓	✓	✓	BESIII23 [10]	5.7–8.4
	✓	✓		BESIII21 [19]	5.7–9.1
	✓			CLEO [31, 32]	
$\Xi^-$	✓			BESIII23 [11]	9.6–23.5
	✓			BESIII20 [21]	16.1–21.2

# CST compared to Recent Hyperon FF data

Use S.Pacetti, R. Baldini Ferroli and E. Tomasi-Gustafsson, Phys. Rept. 550-551,1 (2015):

Unitarity and Analyticity demand that for  $q^2 \rightarrow \infty$

$$G_M(q^2) \simeq G_M^{\text{SL}}(-q^2),$$

$$G_E(q^2) \simeq G_E^{\text{SL}}(-q^2).$$

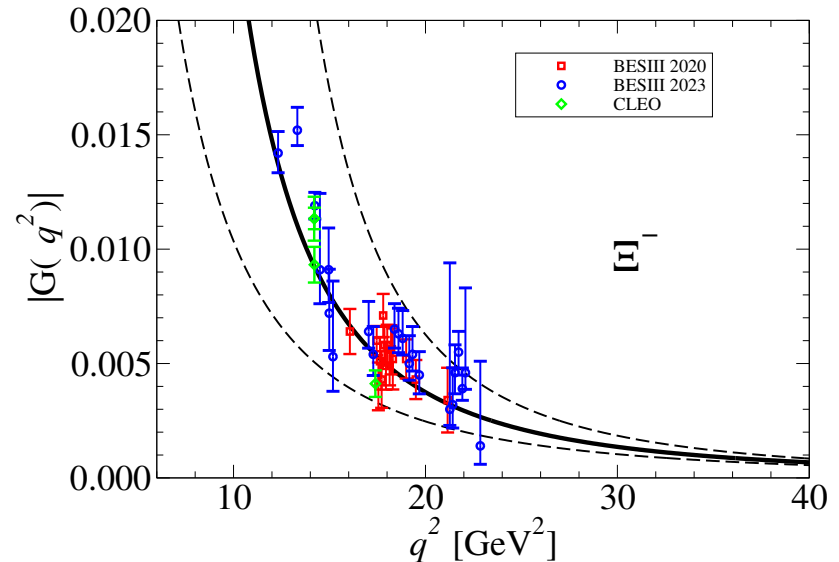
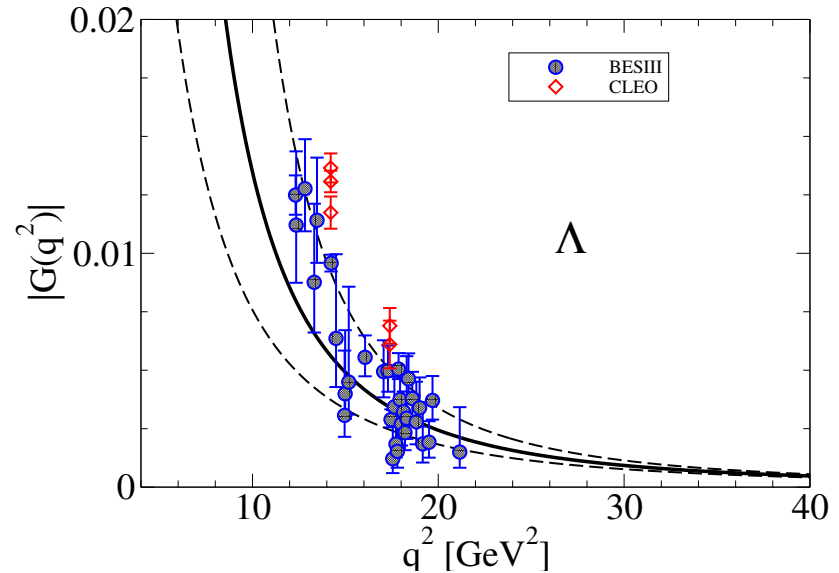
Guidance for determination of onset of "reflection" symmetry

Uncertainty:

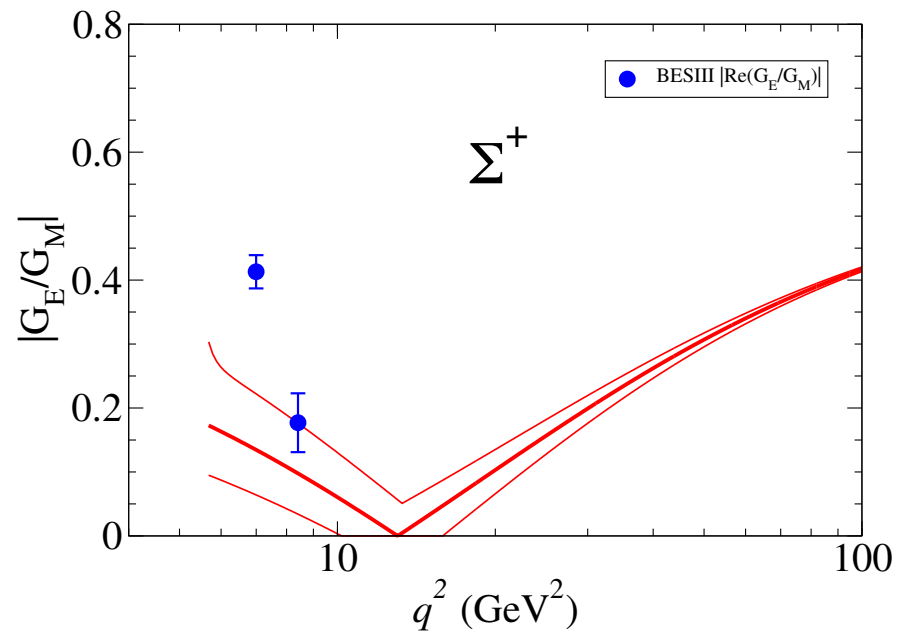
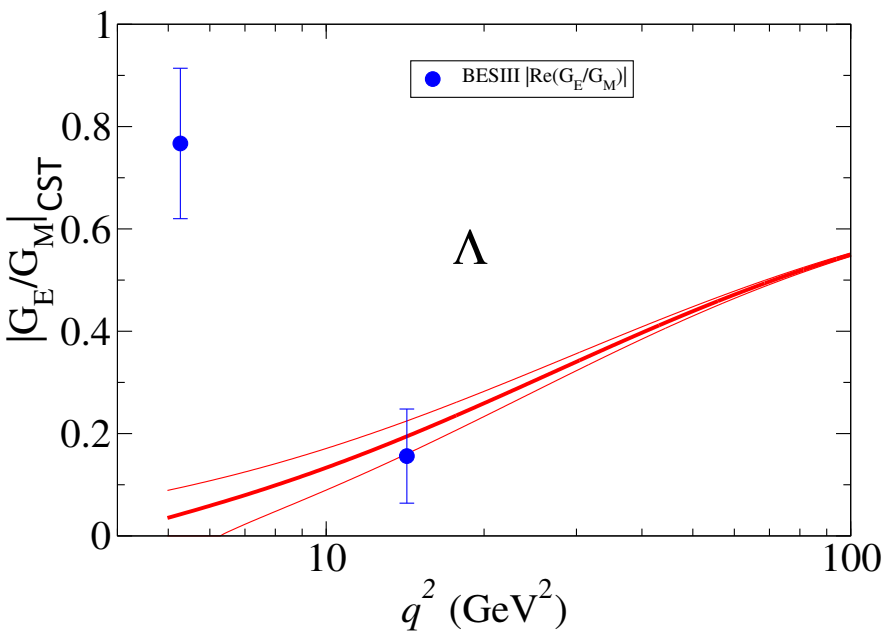
Full line:  $G(q^2) = G(2M^2 - q^2)$

Dashed lines:  $G(q^2) = G(4M^2 - q^2)$

$G(q^2) = G(-q^2)$



$$\left| \operatorname{Re} \left( \frac{G_E}{G_M} \right) \right| = \frac{|G_E|}{|G_M|} |\cos(\Delta\Phi)|,$$



# Summary

---

**CST** phenomenological ansatz for the baryon wave functions describes different excited states of the nucleon, with a variety of spin and orbital motion.

- 1** Descriptions consistent with experimental data at high  $Q^2=-q^2$ .
- 2** Model made consistent with LQCD in the large pion mass regime (through VMD).
- 3** Spacelike e.m. transition FFs for:  
 **$N^*(1440)$ ,  $N^*(1520)$ ,  $N^*(1535)$ , ...**, baryon octet, etc.
- 4** Extension to timelike e.m. transition FFs for dilepton mass spectrum and decay widths, and hyperon form factors; predictive power demonstrated.
- 5** Investigate low  $q^2$  momentum transfer region:  
Determine timelike form factors of higher mass states for knowledge of proton and the neutron electromagnetic couplings ( $q^2=0$ ) in the transitions.

Our approach is phenomenological,  
in the best tradition of the beginnings of Hadron Physics

“Murray looked at two pieces of paper, looked at me and said  
***‘In our field it is customary to put theory and experiment  
on the same piece of paper’.***”

Memories of Murray and the Quark Model  
George Zweig, *Int.J.Mod.Phys.A*25:3863-3877,2010



Zweig quark or the constituent quark





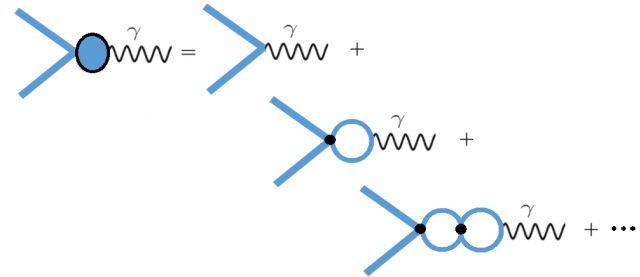
Back up slides

$$f(Q^2) = e + gB(Q^2)e + gB(Q^2)gB(Q^2)e + \dots = e + \frac{gB(Q^2)e}{1 - gB(Q^2)}$$

$$\text{if } gB(Q^2) = \frac{\lambda^2}{\Lambda^2 + Q^2}, \text{ then } f(Q^2) = e + \frac{\lambda^2 e}{\Lambda^2 - \lambda^2 + Q^2}$$

$$f_{1\pm} = \lambda_{\pm} + \frac{1 - \lambda_{\pm}}{1 + Q_0^2/m_v^2} + \frac{c_{\pm} Q_0^2/M_h^2}{(1 + Q_0^2/M_h^2)^2}$$

$$f_{2\pm} = \kappa_{\pm} \left( \frac{d_{\pm}}{1 + Q_0^2/m_v^2} + \frac{(1 - d_{\pm})}{1 + Q_0^2/M_h^2} \right)$$



$$\Gamma_{\mu}(p, Q) = \gamma_{\mu} + \int \frac{d^4 q}{(2\pi)^4} K(p, q, Q) S(q + \eta Q) \Gamma_{\mu}(q, Q) S(q - \eta Q)$$

To parametrize the current use **Vector Meson Dominance at the quark level** a truncation to the rho and omega poles of the full meson spectrum contribution to the quark-photon coupling.

**4** parameters

$$\frac{m_\nu^2}{m_\nu^2 - q^2} \rightarrow \frac{m_\nu^2}{m_\nu^2 - q^2 - im_\nu \Gamma_\nu(q^2)},$$

$$\Gamma_\rho(q^2) = \Gamma_\rho^0 \frac{m_\rho^2}{q^2} \left( \frac{q^2 - 4m_\pi^2}{m_\rho^2 - 4m_\pi^2} \right)^{\frac{3}{2}} \theta(q^2 - 4m_\pi^2), \quad (4.7)$$

where  $\Gamma_\rho^0 = 0.149$  GeV.

For the application in this paper, however, we also have to include the  $\omega$  pole. To this end, the function  $\Gamma_\omega(q^2)$  will include the decays  $\omega \rightarrow 2\pi$  (function  $\Gamma_{2\pi}$ ) and  $\omega \rightarrow 3\pi$  (function  $\Gamma_{3\pi}$ ). The case  $\omega \rightarrow 3\pi$  can be interpreted as the process  $\omega \rightarrow \rho\pi \rightarrow 3\pi$ , and therefore we decomposed  $\Gamma_\omega(q^2)$  into [44]

$$\Gamma_\omega(q^2) = \Gamma_{2\pi}(q^2) + \Gamma_{3\pi}(q^2), \quad (4.8)$$

$$\Gamma_{2\pi}(q^2) = \Gamma_{2\pi}^0 \frac{m_\omega^2}{q^2} \left( \frac{q^2 - 4m_\pi^2}{m_\omega^2 - 4m_\pi^2} \right)^{\frac{3}{2}} \theta(q^2 - 4m_\pi^2), \quad (4.9)$$

where  $\Gamma_{2\pi}^0 = 1.428 \times 10^{-4}$  GeV. Note that  $\Gamma_{2\pi}$  is similar to the function  $\Gamma_\rho$  except for the constant  $\Gamma_{2\pi}^0$  (about  $10^3$  smaller) and the mass. For the function  $\Gamma_{3\pi}$  we use the result from Ref. [44]

$$\Gamma_{3\pi}(q^2) = \int_{9m_\pi^2}^{(q-m_\pi)^2} ds \mathcal{A}_\rho(s) \bar{\Gamma}_{\omega \rightarrow \rho\pi}(q^2, s), \quad (4.10)$$

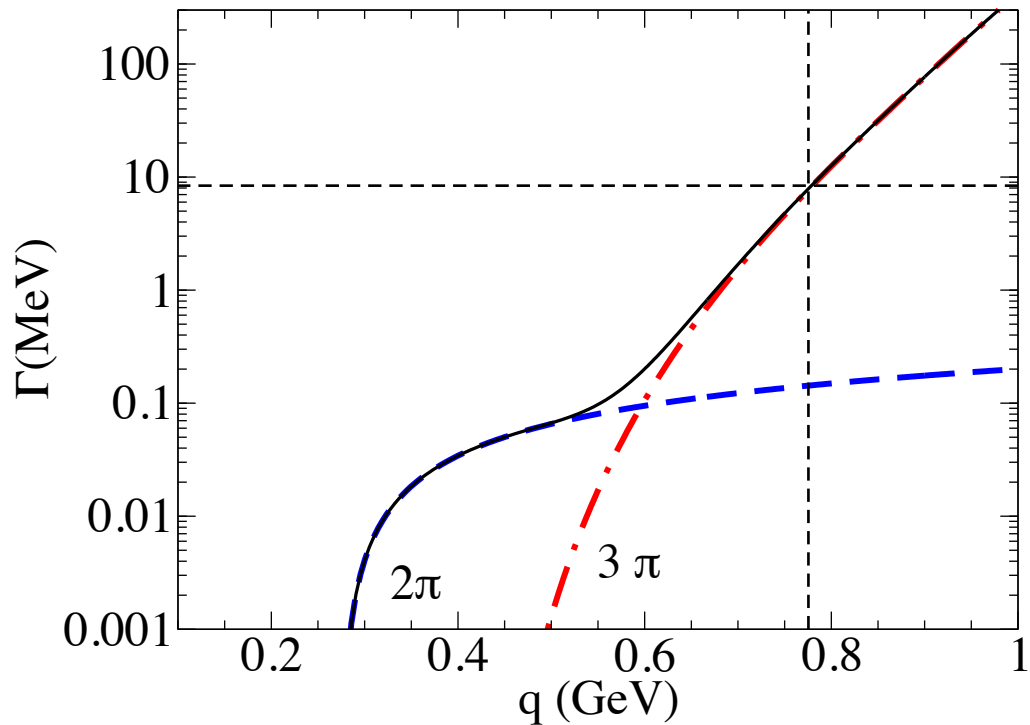


FIG. 1:  $\Gamma_\omega$  as a function of  $q$ . The  $2\pi$ ,  $3\pi$  channels are indicated by the long-dashed and dotted-dashed lines respectively. The solid line represents the sum of the two channels. The short-dashed vertical and horizontal lines indicate the  $\omega$  mass point and the  $\omega$ -physical width (8.4 MeV).

# Extension to Strangeness in the timelike region

CST seems to work well at large  $Q^2$ .

$$e^+e^- \rightarrow \gamma^* \rightarrow B\bar{B}$$

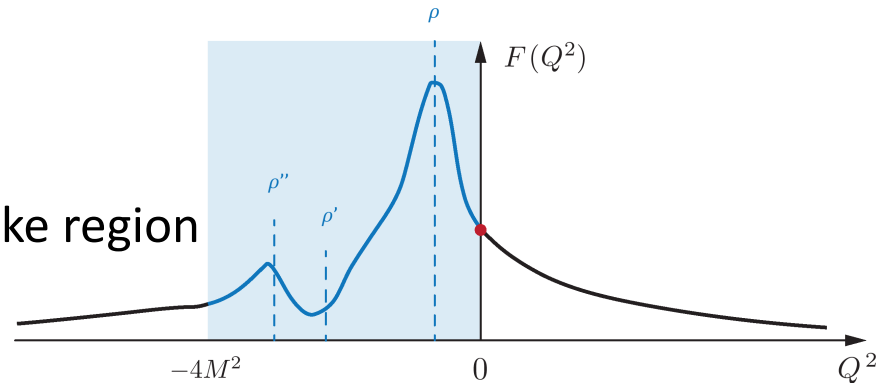
Use S.Pacetti, R. Baldini Ferroli and E. Tomasi-Gustafsson,  
 Phys. Rept. 550-551,1 (2015).

Unitarity and Analyticity  
 demand that for  $q^2 \rightarrow \infty$

Reflection symmetry sets in,  
 implying real form factor as in the space like region

$$G_M(q^2) \simeq G_M^{\text{SL}}(-q^2),$$

$$G_E(q^2) \simeq G_E^{\text{SL}}(-q^2).$$



Effective Form factor  
 that gives the  
 integrated cross  
 section

$$|G(q^2)|^2 = \left(1 + \frac{1}{2\tau}\right)^{-1} \left[ |G_M(q^2)|^2 + \frac{1}{2\tau} |G_E(q^2)|^2 \right]$$

$$= \frac{2\tau |G_M(q^2)|^2 + |G_E(q^2)|^2}{2\tau + 1}.$$

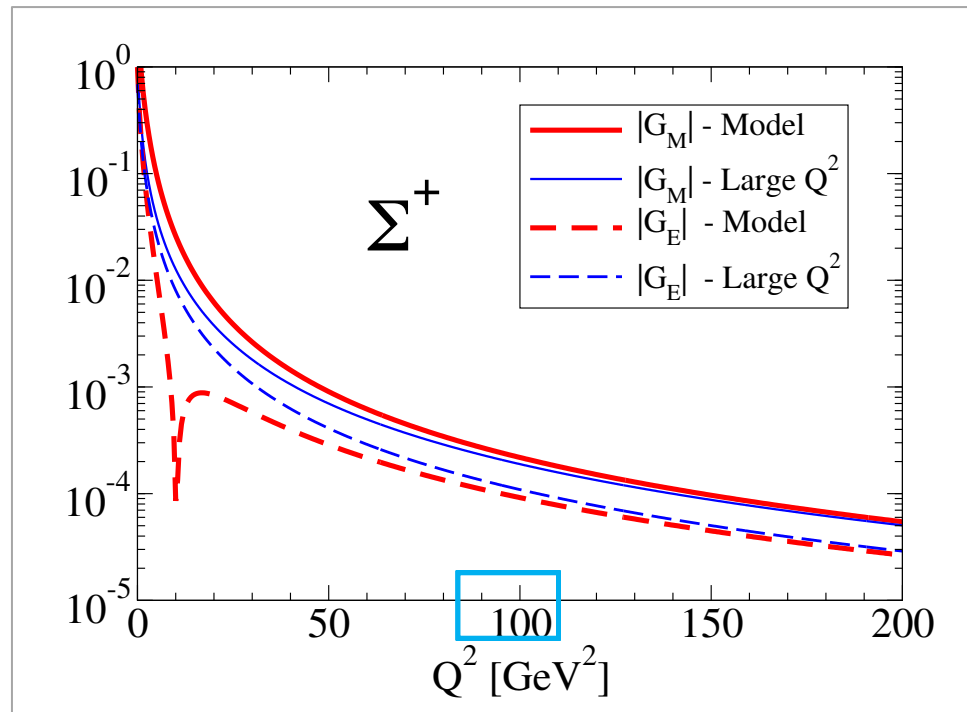
$$\tau = \frac{q^2}{4M_B^2}$$

# Asymptotic behavior reached at energies higher than reflection property

$$e^+e^- \rightarrow \gamma^* \rightarrow B\bar{B}$$

Guidance for determination of onset of perturbative QCD falloffs:

$$G_M \propto 1/q^4 \text{ and } G_E \propto 1/q^4.$$



Perturbative QCD limit is way above the region where reflection symmetry starts to be valid (**100 GeV $^2$  versus 10 GeV $^2$** )

$$\Gamma_{\gamma^* N}(q; W) = \frac{\alpha}{16} \frac{(W + M)^2}{M^2 W^3} \sqrt{y_+ y_-} |G_T(q^2, W)|^2$$

$$|G_T(q^2; M_\Delta)|^2 = |G_M^*(q^2; W)|^2 + 3|G_E^*(q^2; W)|^2 + \frac{q^2}{2W^2} |G_C^*(q^2; W)|^2$$

$$y_\pm = (W \pm M)^2 - q^2$$

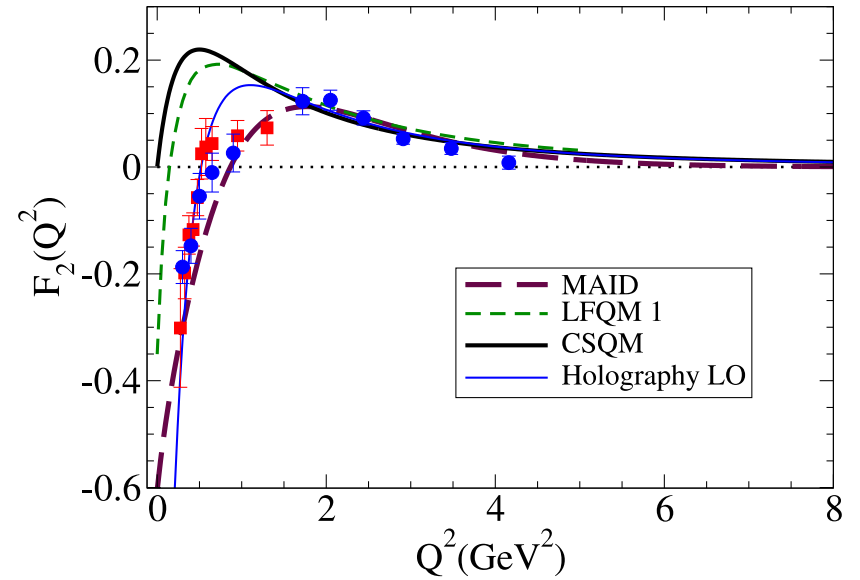
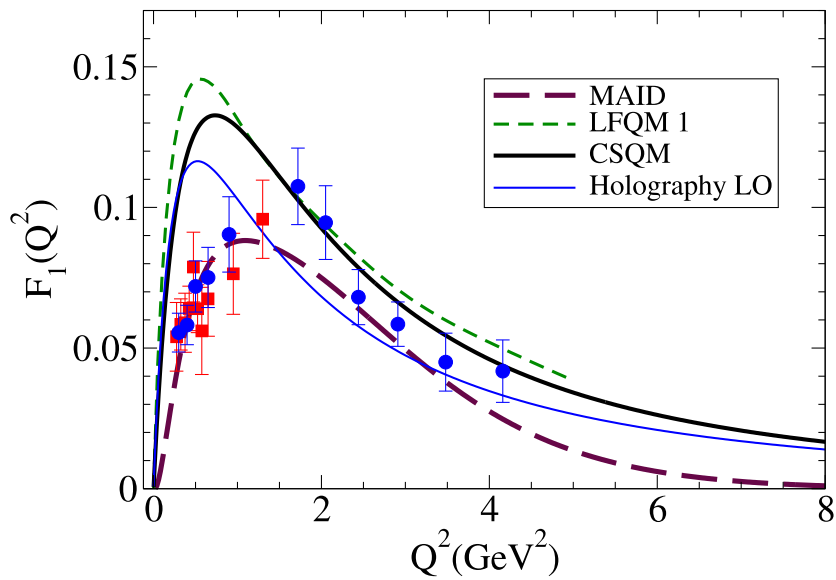
$$\Gamma_{\gamma N}(W) \equiv \Gamma_{\gamma^* N}(0; W)$$

$$\Gamma_{e^+ e^- N}(W) = \frac{2\alpha}{3\pi} \int_{2m_e}^{W-M} \Gamma_{\gamma^* N}(q; W) \frac{dq}{q}$$



# $N \rightarrow N^*(1440)$ TFFs

$J^P=1/2^+ \quad I=1/2$



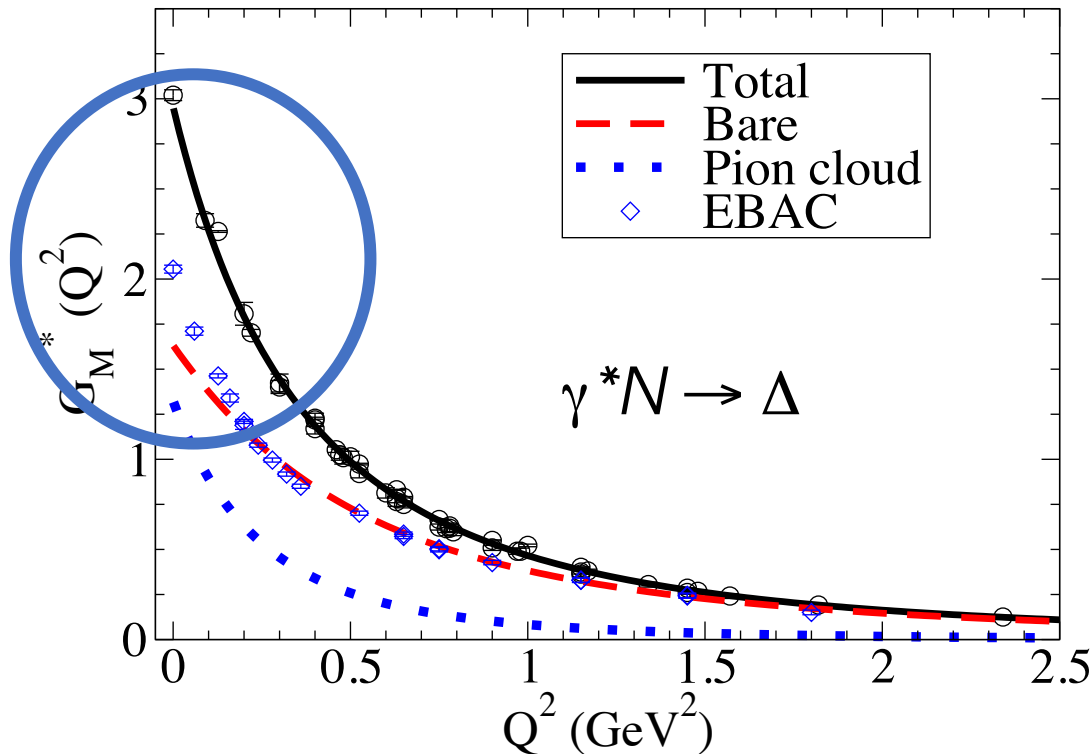
# Model independent feature (Covariant Spectator Theory)



**Missing strength of**  $G_M$  at the origin.

Separation between quark core and pion cloud seems to be supported by experiment.

$$|G_M^* = G_M^B + G_M^\pi$$



**CST**© 2009

**Bare quark core:**

- dominates in the large  $Q^2$  region.
- agrees with other calculations (“EBAC”) with pion couplings switched off.

# Transition E.M. Current

---

$$\gamma N \rightarrow \Delta$$

$$\Gamma^{\beta\mu}(P, q) = [G_1 q^\beta \gamma^\mu + G_2 q^\beta P^\mu + G_3 q^\beta q^\mu - G_4 g^{\beta\mu}] \gamma_5$$

- Only 3  $G_i$  are independent:  
E.M. Current has to be conserved

$$q^\mu \Gamma_{\beta\mu} = 0 \quad \longrightarrow$$

$G_M, G_E, G_C$  Scadron-Jones popular choice.

## Transition E.M. Current

---

$$\gamma N \rightarrow \Delta$$

$$\Gamma^{\beta\mu}(P, q) = [G_1 q^\beta \gamma^\mu + G_2 q^\beta P^\mu + G_3 q^\beta q^\mu - G_4 g^{\beta\mu}] \gamma_5$$

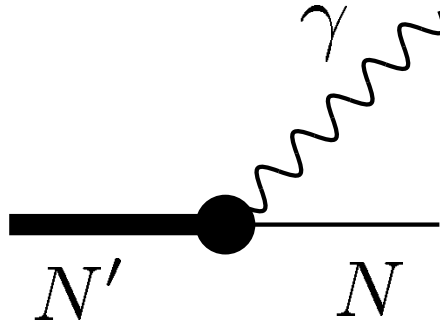
- Only 3  $G_i$  are independent:  
E.M. Current has to be conserved

$$q^\mu \Gamma_{\beta\mu} = 0 \quad \longrightarrow$$

$G_M, G_E, G_C$  Scadron-Jones popular choice.

- Only finite  $G_i$  are physically acceptable.

# Extension to Timelike



*R* rest frame

$$P_R = (W, 0, 0, 0); \quad P_N = (E_N, 0, 0, -|\mathbf{q}|); \quad q = (\omega, 0, 0, |\mathbf{q}|)$$

Timelike  $q^2 > 0$

$$\omega = \frac{W^2 - M^2 + q^2}{2W}$$

$$|\mathbf{q}|^2 = \frac{[(W + M) - q^2][(W - M)^2 - q^2]}{4W^2}$$

$$E_N = \frac{W^2 + M^2 - q^2}{2W}$$

Spacelike  $-q^2 = Q^2 > 0$

$$\omega = \frac{W^2 - M^2 - Q^2}{2W}$$

$$|\mathbf{q}|^2 = \frac{[(W + M) + Q^2][(W - M)^2 + Q^2]}{4W^2}$$

$$E_N = \frac{W^2 + M^2 + Q^2}{2W}$$

TL:  $q^2 \leq (W - M)^2$

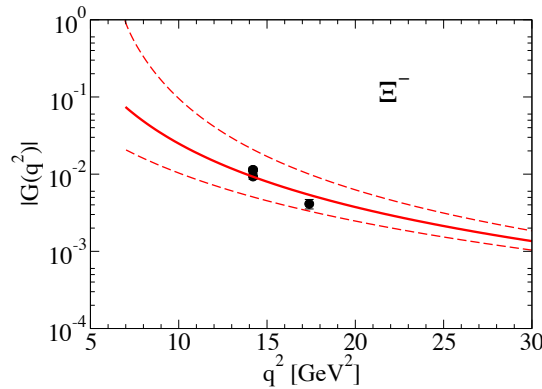
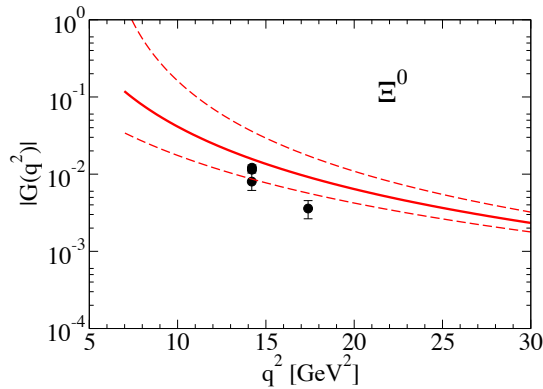
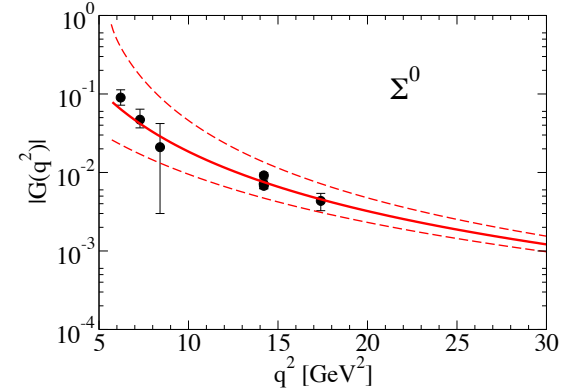
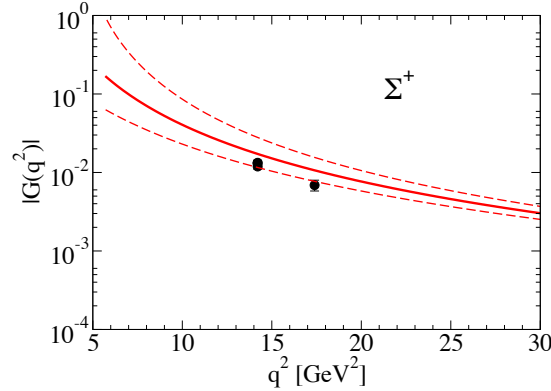
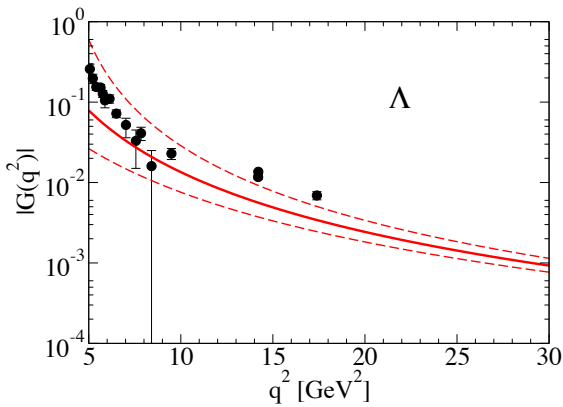
$W \geq M$

Transition form factors in the timelike region are restricted to a given kinematic region that depends on the varying resonance mass  $W$ .

# Extension to Strangeness in the timelike region

$$e^+e^- \rightarrow \gamma^* \rightarrow B\bar{B}$$

Data from Babar, CLEO, BESIII



$$G_M(q^2) \simeq G_M^{\text{SL}}(-q^2),$$

$$G_E(q^2) \simeq G_E^{\text{SL}}(-q^2).$$

Uncertainty bar:

Full line:  $G(q^2) = G(2M^2 - q^2)$

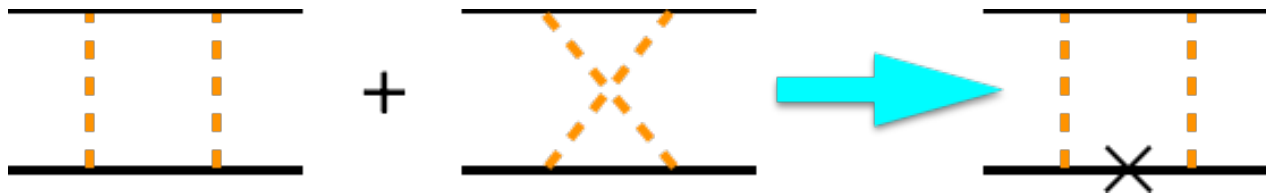
Dashed lines:  $G(q^2) = G(4M^2 - q^2)$   
 $G(q^2) = G(-q^2)$

Guidance for determination of onset of "reflection" symmetry

	$G$	$\frac{G_E}{G_M}$	$\Delta\Phi$	Experiment	$q^2$ range (GeV <sup>2</sup> )
$\Lambda$	✓			BESIII23 [13]	5.0–8.7
	✓			BESIII21 [16]	12.3–21.2
	✓			BaBar06 [8], CLEO [31, 32]	
		✓	✓	BESIII22 [15]	14.2
		✓	✓	BESIII23 [14]	13.8 †
	✓	✓	✓	BESIII19 [22]	5.7
	✓	✓		BaBar07 [9]	
$\Sigma^0$	✓			BaBar06 [8]	
$\Sigma^+$	✓	✓	✓	BESIII23 [10]	5.7–8.4
	✓	✓		BESIII21 [19]	5.7–9.1
	✓			CLEO [31, 32]	
$\Sigma^-$	✓			BESIII21 [19]	5.7–9.1

# CST<sup>©</sup> covariant Spectator Theory

- Formulation in Minkowski space.
- Motivation is partial cancellation



- Manifestly covariant, although only three-dimensional loop integrations.

$$\int_k = \int \frac{d^3\mathbf{k}}{2E_D(2\pi)^3}$$

- Provides wave functions from covariant vertex with simple transformation properties under Lorentz boosts, appropriate angular momentum structures and smooth non-relativistic limit.



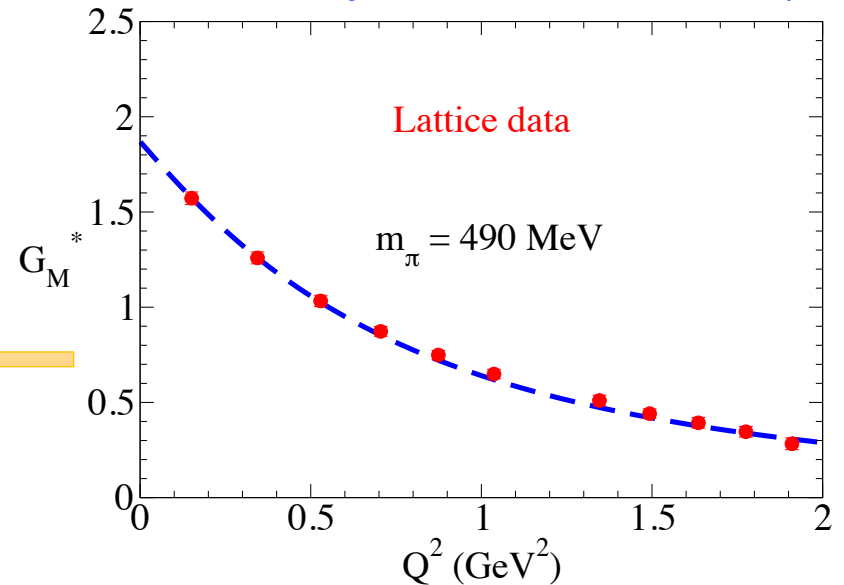
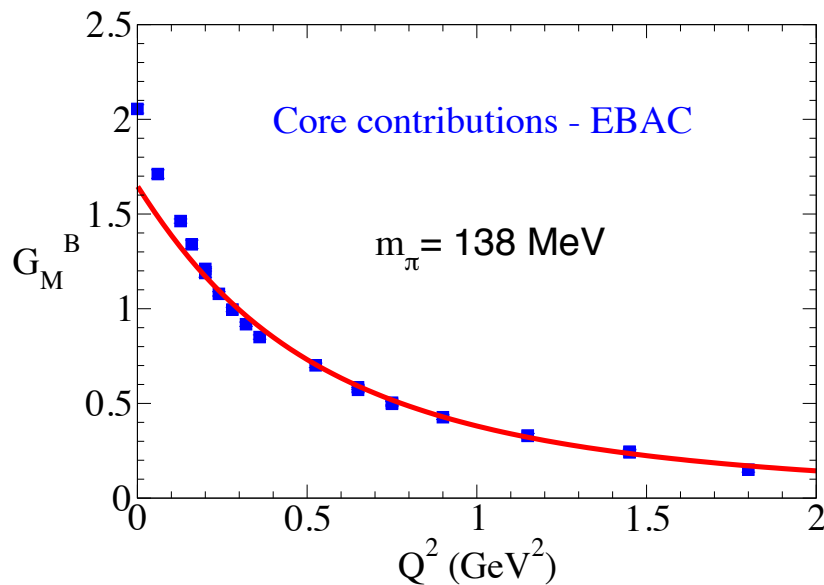
$$\gamma N \rightarrow \Delta$$

## Connection to Lattice QCD

To control model dependence:

CST model and LQCD data are made **compatible**.

G. Ramalho and M. T. Peña, Phys. Rev. D 80, 013008 (2009)

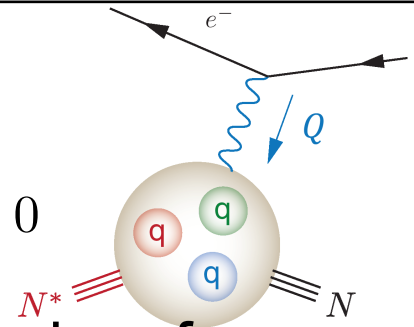


Model (no pion cloud) valid for lattice pion mass regime.

No refit of wave function scale parameters for the physical pion mass limit.

# E.M. Current and TFF near the photon point

Pseudo Threshold PT  $Q_0^2 = -(M_R - M_N)^2 ; |\vec{Q}| = 0$

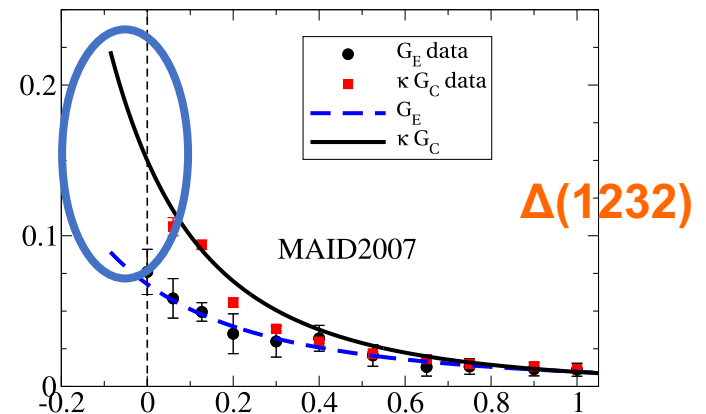


An accident of the definition of the Jones and Scadron form factors:

$$G_E(PT) = \frac{M_R - M}{2M_R} G_C(PT)$$

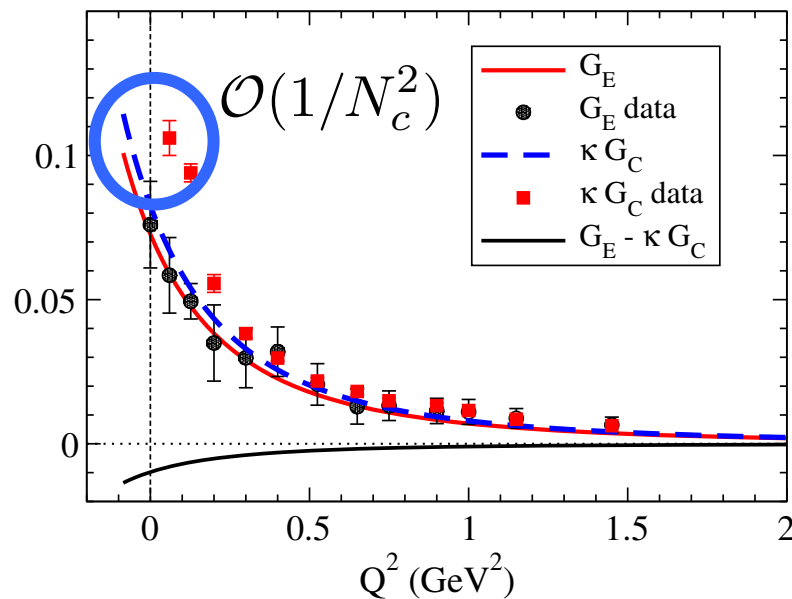
A form of the “Siegert condition”!  
This is implied by orthogonality of states.

If data analysis proceed through helicity amplitudes this behavior may be missed.



Large  $N_C$  limit and SU(6) quark models:

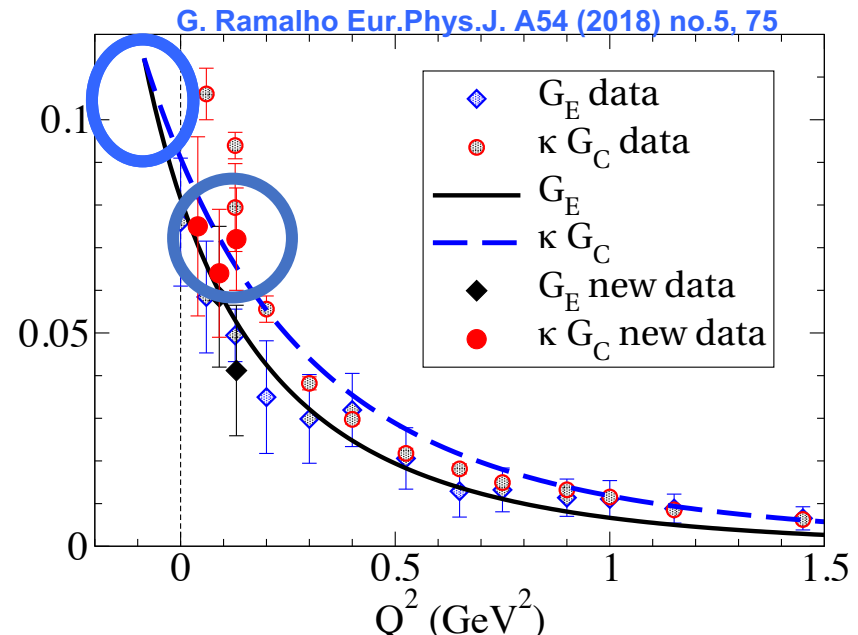
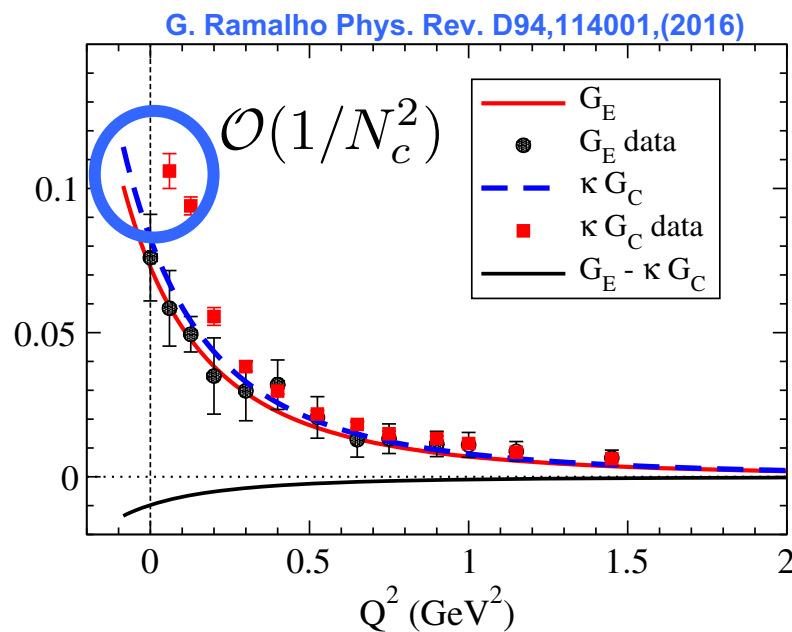
- Suggest that pion cloud effects for  $G_E$  and  $G_C$  generate deviations from the Siegert condition of the order  $\mathcal{O}(1/N_c^2)$  and do not agree to data at low  $Q^2$ .



Large  $N_C$  limit and SU(6) quark models:

- Suggest that pion cloud effects for  $G_E$  and  $G_C$  generate deviations from the Siegert condition of the order  $\mathcal{O}(1/N_c^2)$  and do not agree to data at low  $Q^2$ .

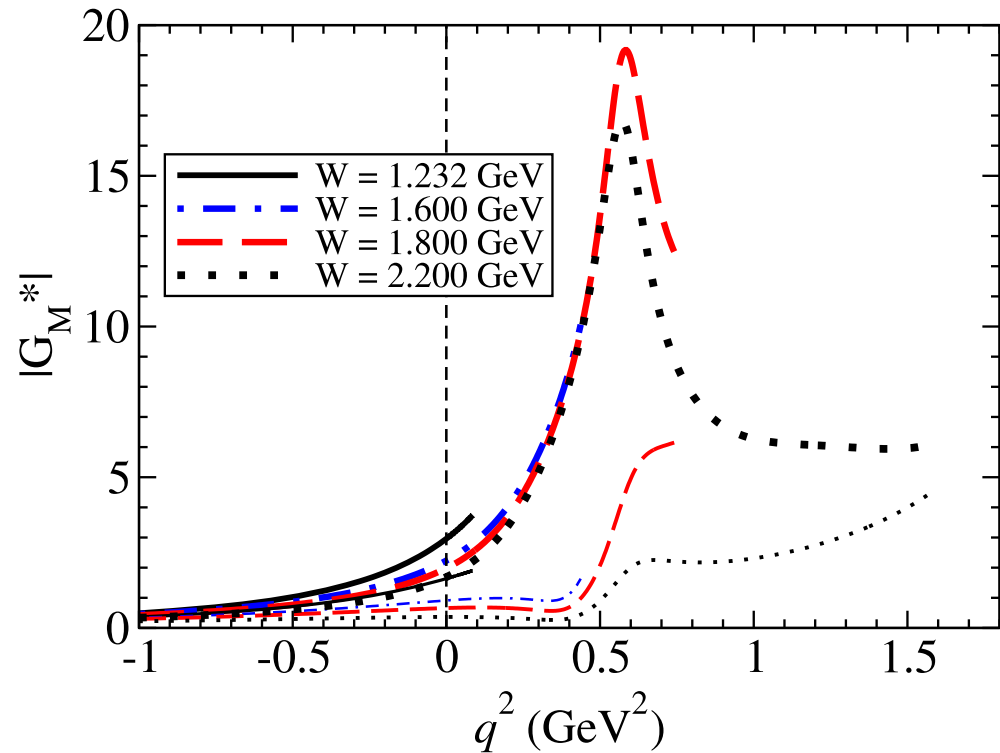
Corrected parametrization with deviations  $\mathcal{O}(1/N_c^4)$  generated agreement with 2017 JLAB data

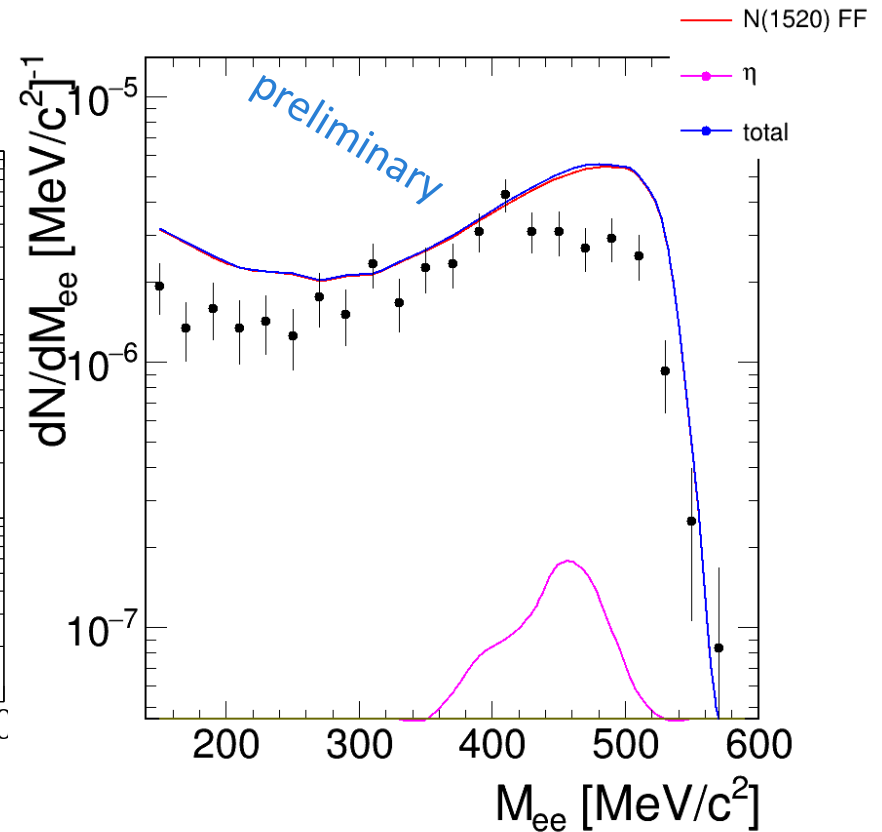
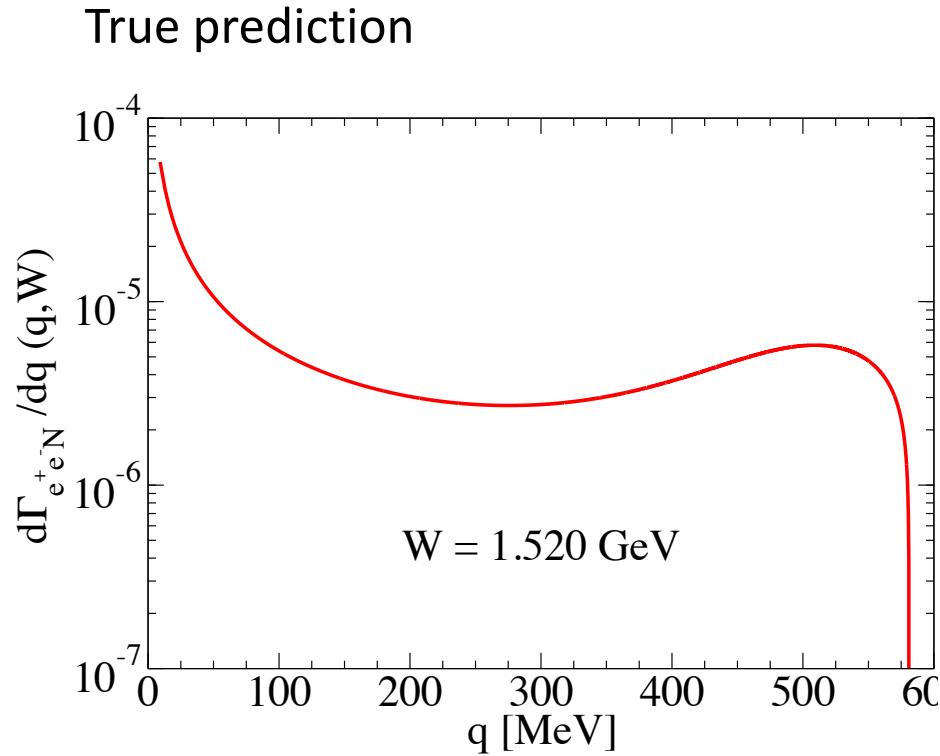


# Extension to Timelike

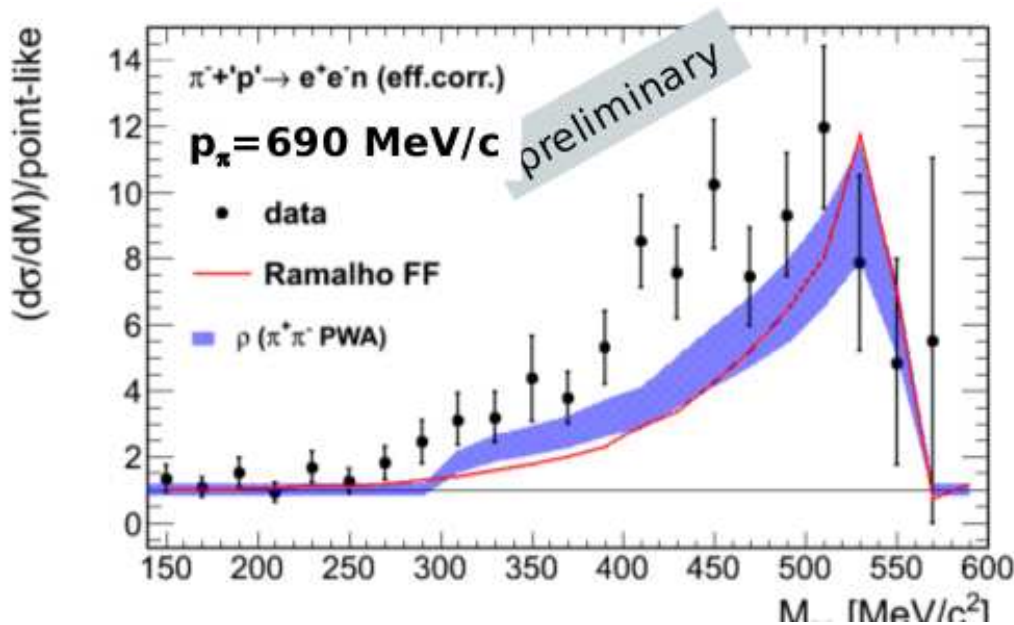
$$\gamma N \rightarrow \Delta$$

- Extension to higher  $W$  shows effect of the rho mass pole
- In that pole region small bare quark contribution (thin lines)





Effect of dependence of e.m. coupling with  $W$       True prediction



B. Ramstein, NSTAR2019

HADES Collaboration

Ratio to pointlike case

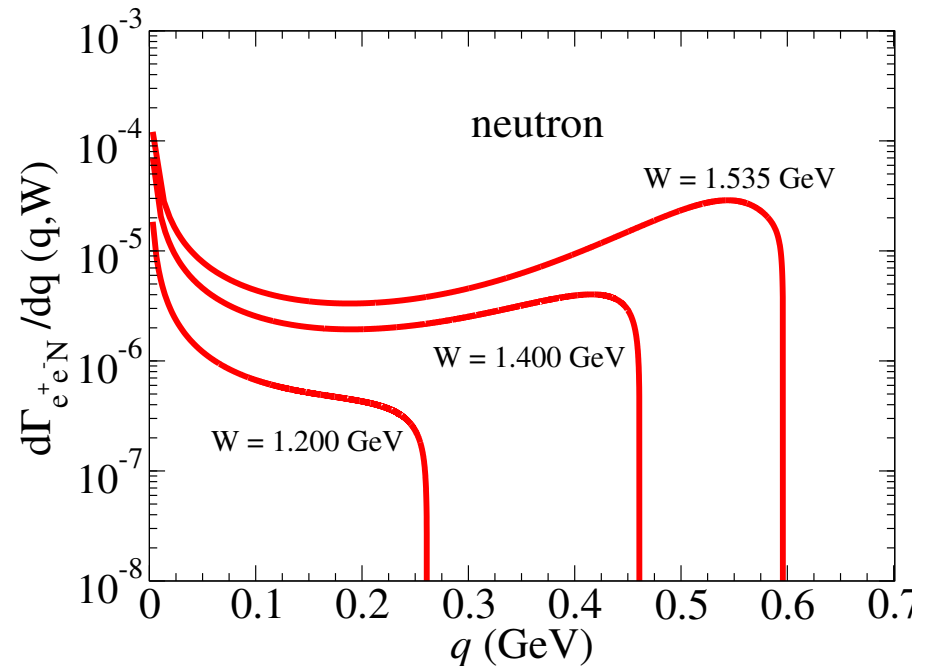
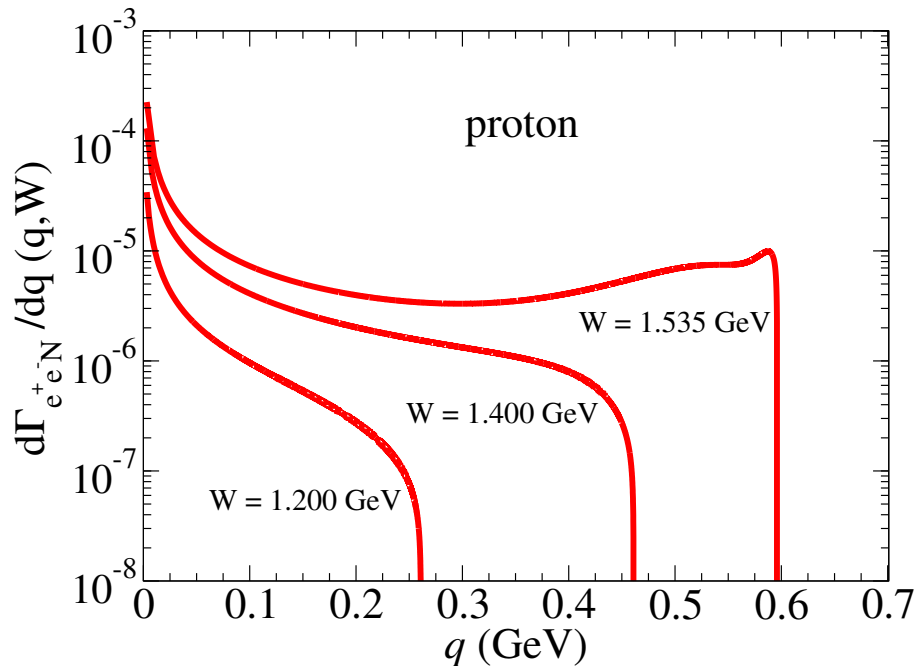
# Crossing the boundaries

# N\*(1535) Dalitz decay

$$\Gamma_{\gamma^* N}(q, W) = \frac{\alpha}{2W^3} \sqrt{y_+ y_-} y_+ B \|G_T(q^2, W)\|^2,$$

$$\|G_T(q^2, W)\|^2 = |G_E(q^2, W)|^2 + \frac{q^2}{2W^2} |G_C(q^2, W)|^2$$

$$\frac{d\Gamma_{e^+e^-N}}{dq}(q, W) = \frac{2\alpha}{3\pi q^3} (2\mu^2 + q^2) \sqrt{1 - \frac{4\mu^2}{q^2}} \Gamma_{\gamma^* N}(q, W),$$

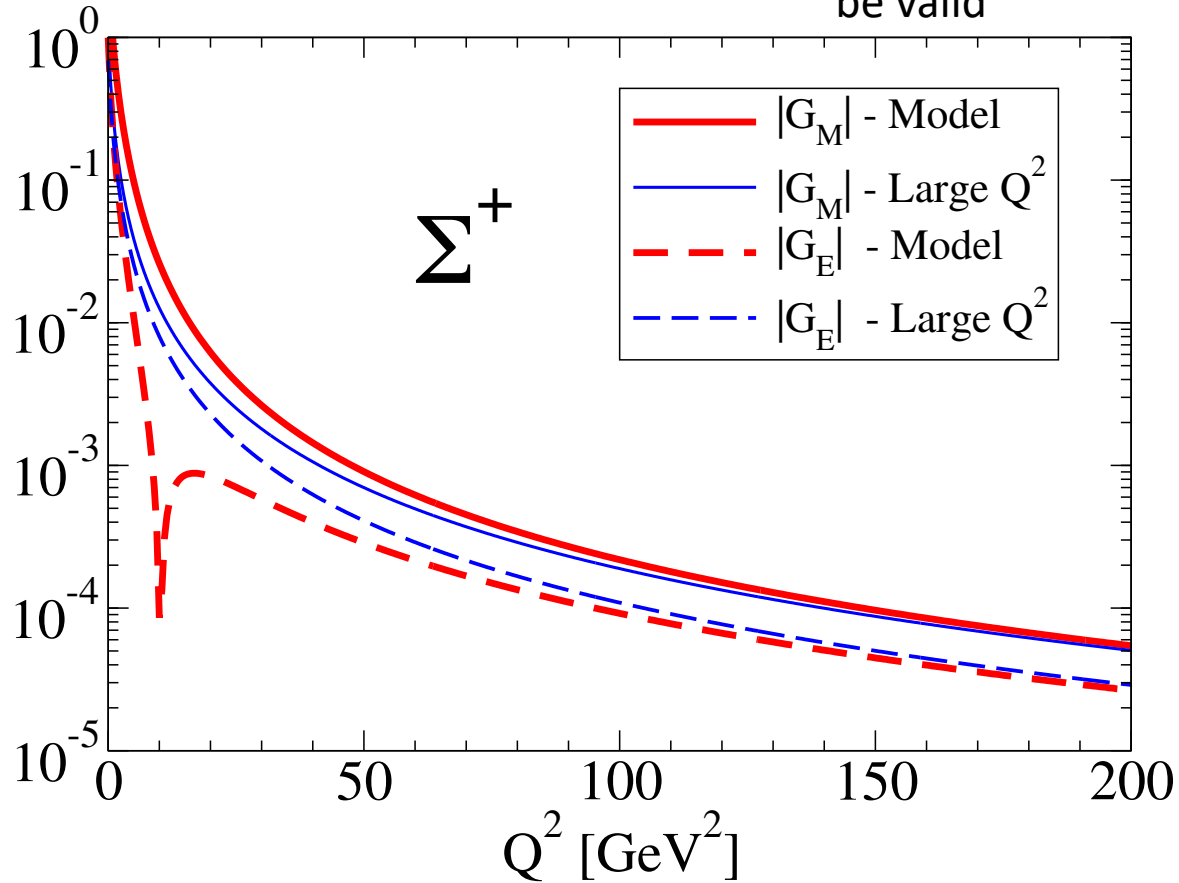




# Asymptotic behavior

$$e^+e^- \rightarrow \gamma^* \rightarrow B\bar{B}$$

Perturbative QCD limit is way above the region where reflection symmetry starts to be valid

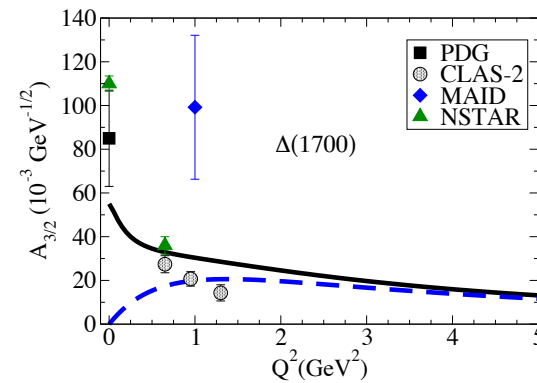
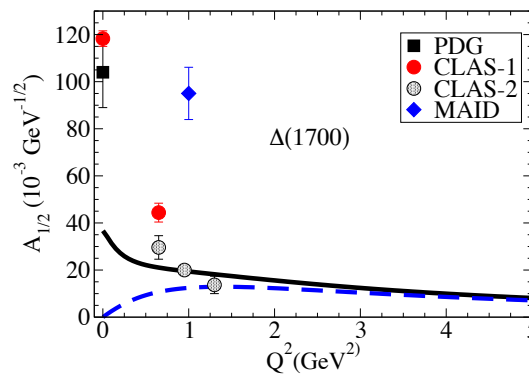
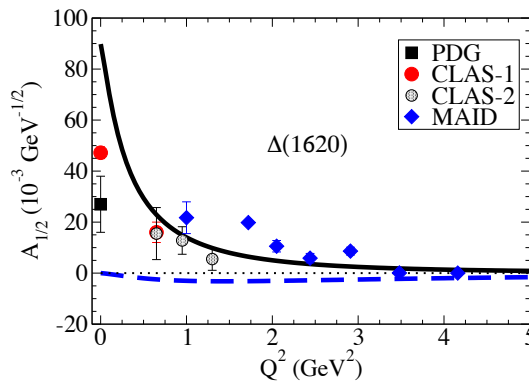
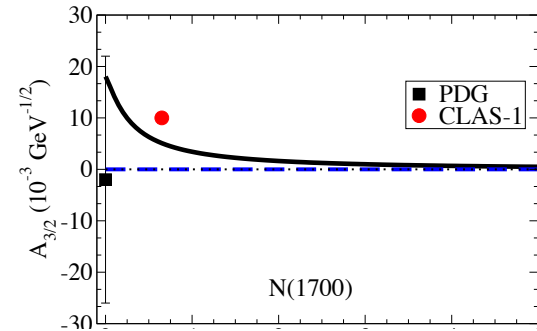
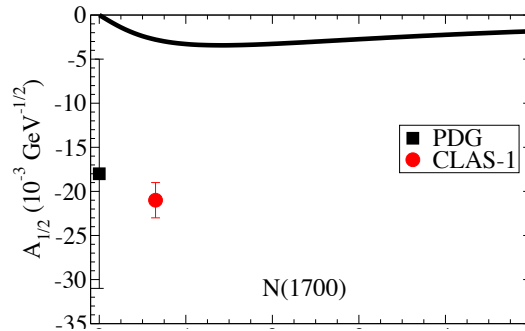
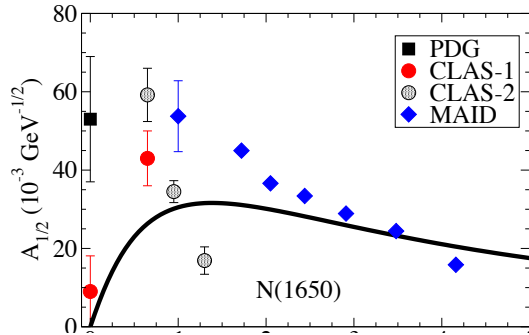


# Predictive power:

D13(J=3/2-) **S11**(J=1/2-) (I=1/2) are part of a large supermultiplet (SU(6) spin-flavor with O(3) symmetry)

S. Capstick and W. Roberts,  
Prog. Part. Nucl. Phys. 45,  
S241 (2000);  
V. D. Burkert et al.  
Phys. Rev. C 67, 035204 (2003).

**Input:** N(1520), N(1535); **Output:** N(1650), N(1700),  $\Delta$ (1620),  $\Delta$ (1700)  
D13                      **S11**                      **S11**                      D13                      **S31**                      D33



Bare quark CST description  
expected to work well  
in high  $Q^2$  region!

G. Ramalho, PRD 90, 033010 (2014)